

Numerical Analysis of IEEE Project 1597.1 Validation Problems

G.Antonini, M. Italiani, A.Orlandi

UAq EMC Laboratory
Dept. of Electrical Engineering
University of L'Aquila
L'Aquila
Italy

1. INTRODUCTION

There is no doubt that the actual computational electromagnetic (CEM) scientific community is concerned about the validation and verification (V&V) [1] of the results generated by the numerical simulations. This attitude is justified by the need for reliable technologies and repeatable methods for assessing the electromagnetic performances of complex systems and/or devices. This is the reason of the IEEE Project 1597.1 aiming to develop standards for CEM computer modeling and technique validation [2,3]. Inside of this Project, a number of standard electromagnetic compatibility (EMC) and signal integrity (SI) problems have been identified and translated into models to be analyzed by means of different CEM techniques.

In this work, three of them have been selected and used to analyze the impact of the variation of some geometrical properties or simulation parameters' settings on final results. They can be, for example, size of aperture, number of aperture, component placement on PCBs, mesh size and density, etc. The three benchmarks investigated cover a range of applications from a standard shielding problem, to a typical PCB structure up to a meandered line very often encountered in SI analysis.

In the first benchmark, dealing with the shielding properties of a metallic enclosure, it has been investigated the sensitivity of the numerical outputs to the characteristic of the discretization grid used for the numerical analysis. The second benchmark considers the impact of the correct numerical modelling of the reference plane in a PCB structure when a slot is open in this plane. Finally, the third benchmark looks on how the modelling of the meander, of the reference plane and of the substrate can change the results obtained by numerical analysis.

The numerical simulations have been performed by using CST STUDIO SUITE 2006 [4], a software based on the Finite Integration Technique (FIT) [5].

The Feature Selective Validation (FSV) technique [6,7] is used as conceptual tool for the data comparison between different simulations. This technique is one of those mentioned in the IEEE Project 1597.1. In the next section, the FSV technique is briefly recalled and the main figure of merits used along this paper explained and commented.

2. THE FEATURE SELECTIVE VALIDATION (FSV)

The Feature Selective Validation (FSV) techniques aims to perform the comparison of different datasets by mimic the behaviour of a group of experienced engineers when they perform such a comparison by means of a visual approach. [5],[6].

The FSV method is based on the decomposition of the original data into two parts: amplitude (trend/envelope) data and feature data. The former component accounts for the slowly varying data across the data set and the latter accounts for the sharp peaks and troughs often found in CEM data. The numerical figures of merit obtained as output from the FSV procedure can be converted in a natural language descriptor (excellent, very good, good, fair, poor, very poor comparison). In the two references mentioned above it is described the rigorous theory behind this method. In the following it is only reported the essential meaning of the FSV figures of merit used along the text.

They are:

ADM (Amplitude Difference Measure) and FDM (Feature Difference Measure) which are two figures of goodness-of-fit between the two data set being compared. The former quantifies the comparison of the trends of the two datasets (the slowing varying shapes of the data), the latter quantifies the comparison of the rapidly changing shapes of the data (the features). Their point-by-point numerical values can be converted in a natural language descriptor scale. These single figure goodness-of-fit values combine to give the GDM.

GDM (Global Difference Measure) which is an overall single figure goodness-of-fit between the two data sets being compared. This allows a simple decision to be made about the quality of comparison. This may be numerical or converted to a natural language descriptor (excellent, very good, good, fair, poor, very poor). This is obtained from the overall figures for the two components, the amplitude difference measure and the feature difference measure.

GDMc, ADMc, FDMc which give a probability density function which shows the proportion of the point-by- point analyses of each of the components that falls into the six natural language descriptor categories. These figures of merits (the “c” stands for “confidence”) provides a measure of confidence in the single figure comparison, giving some information as to how much emphasis can be placed on the single figure of merit.

While the mean value of the ADM and FDM (and subsequently the GDM) provides a single figure goodness-of-fit measure, there are two aspects of the confidence histograms that help in the interpretation of the confidence histograms. These are:

1. How concentrated the histogram bars are at one extreme or the other.
2. How dispersed the histogram bars are around the mean value.

Both of these can help in deciding whether it is reasonable to give both the ADM and the FDM a similar level of importance or whether to concentrate more on one or the other.

It has been proposed in [Barcellona 06] that these two elements can be combined by using a Grade-Spread chart which gives a numerical value to the Grade by counting how many categories are required (starting from Excellent) for the cumulative total of the histogram to exceed a given value. A numerical value is given to the Spread by counting how many adjacent categories (starting from the largest) are required to cumulatively exceed a given value. A default value for both the grade and spread has been set at 85% in producing this paper, but this may be varied according to requirements. For example, consider the GDM values of Table I due to the comparison of a pair of data sets.

Table I – Numerical values for GDM

Category	Value
Excellent	0.1
Very Good	0.15
Good	0.3
Fair	0.21
Poor	0.24
Very Poor	0

To obtain the Grade, start with the Excellent category and cumulate a total as categories are added. For an 85% total, the Grade is Excellent – Poor, i.e. 5 categories and therefore a Grade of 5. To obtain the Spread, start with the highest category (in this case Good) and add the adjacent highest values categories to obtain 85%, in this case Good + Fair + Poor + Very Good > 85%, so therefore the Spread is 4. These values can be presented graphically on a Grade-Spread Chart. Where the Grade gives a visual indication of the quality of the comparison and the Spread gives a visual indication of the level of confidence that can be placed on this assessment. It emphasizes that a wide Spread gives a poorer overall quality of result than a wider Grade. This, implemented for the data in Table I gives the chart in Fig. 1a.

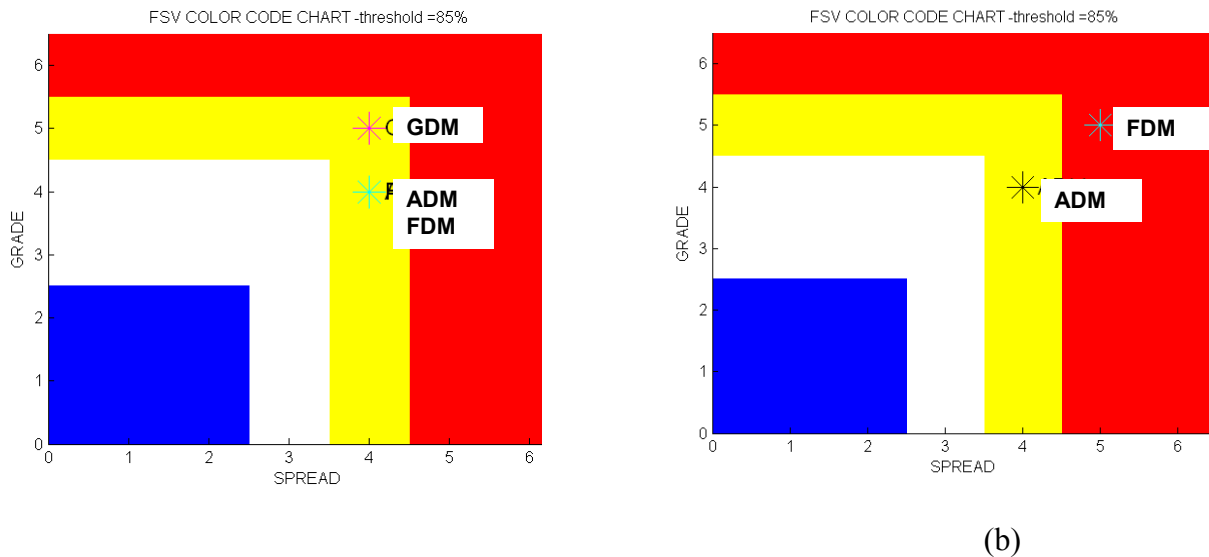


Fig. 1 – (a) Grade-Spread chart of ADM, FDM, GDM for the original data in Table I, (b) Grade-Spread chart of ADM, FDM.

In Fig. 1a ADM and FDM are identical (Yellow) which suggests that they should both be given equal weighting. Subsequently, if this was part of a validation process, movement from Yellow to White or Blue would suggest that there has been an overall improvement in the performance. Considering now the Grade-Spread Chart given in Figure 1b, the figure gives a visual indication of the relative quality of the FDM measure compared with the ADM measure suggesting that in analyzing the data, more emphasis should be given to the ADM. In a practical sense, this may mean that the FDM could be overtly de-rated in discussions about the quality of the comparison or that when looking to improve the simulation or the experiment on which this result is based, analysis of the point-by-point data of the ADM could be considered in preference to the GDM or ADM and

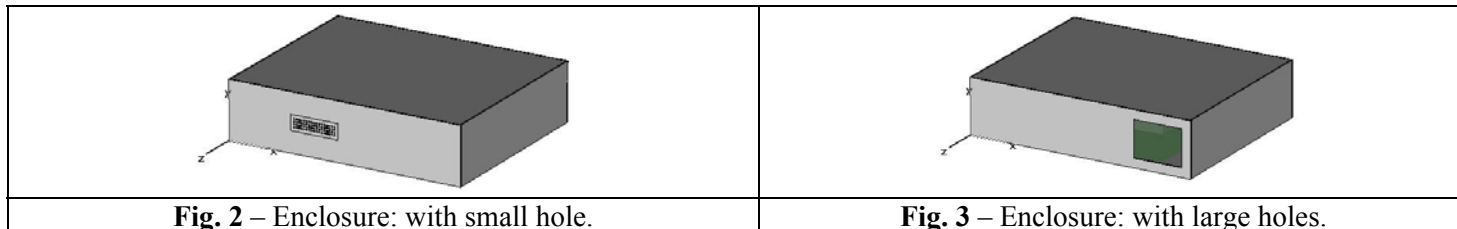
FDM together. In the next chapters, some IEEE Project 1597.1 models will be considered and analyzed.

3. A SHIELDING STANDARD PROBLEM

Shielding effectiveness of an enclosure is a complex matter, in which a lot of different phenomena are involved; for example, electrical and geometrical parameters of the material of the walls, apertures and grids, joints and contacts (connections) (including the use of gaskets, springs, overlaps,...), internal and external cabling and cable feed-through or connectors, and internal boards and backpanels. In most cases, the total shielding effectiveness is determined by the combination of all these effects, some with greater impact than others. As a consequence, determining the shielding effectiveness of a real enclosure is not a simple matter. In order to investigate the effects of simulation settings on numerical results, a complex metal enclosure has been defined, as is shown in Fig. 2. This enclosure includes an internal source, and apertures with different holes sizes.

They have been considered the enclosure in two different configurations: with small holes (see Fig. 2) and with a single large hole as in Fig. 3.

The aim is to compute and compare the magnitude of the electric field at a distance of 3 m by front side of the enclosures for different mesh settings. For both cases different mesh settings have been used and then the comparison of the results varying the mesh are shown. The detailed description of the whole system follows below.



The geometrical dimensions of the entire structure are shown in Fig. 4. The analysis has been performed in the frequency range 0.1GHz - 2GHz.

Enclosure Dimensions and Materials (see Fig. 4):

The enclosure is 370 mm x 90 mm x 300 mm (x , y , z axis); walls' thickness is 2 mm; all enclosure walls are made up of Perfect Electric Conductors (PEC).

Aperture Dimensions (see Fig. 4):

The large hole have sizes 80 mm x 60 mm whose bottom left corner is placed at x = 275mm, y = 15mm. The small holes are organized as a matrix of 4 rows per 17 columns. Each small holes is 2 mm x 2 mm. The holes matrix bottom right corner is placed at x = 104.5 mm, y = 38 mm; the spacing between each small hole is 2 mm.

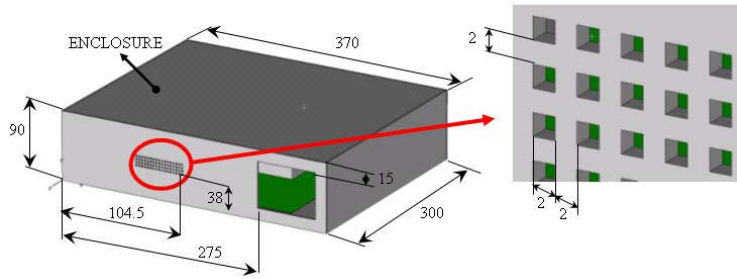


Fig. 4 - Geometrical dimensions of the enclosure; small holes and large hole. (All dimensions is in mm).

ElectroMagnetic (EM) Source Description: Dimensions, Materials and Location (see Fig. 5):

The EM source, i.e. a PCB, is simulated as follows: there is a metal plane in PEC material with dimensions 260 mm x 0.017 mm x 280 mm. Over the metal plane there is a dielectric substrate of FR4 whose dimensions are 260 mm x 0.25 mm x 280 mm; its dielectric permittivity is $\epsilon_r = 4.3$ and no dielectric losses are considered. A trace in PEC material is placed over the dielectric substrate (microstrip configuration); the trace has dimensions 0.4mm x 0.017mm x 280mm and is centered on the plane perpendicular to the slotted panel. A heatsink (solid metal rectangular object) in PEC material of 160 mm x 20 mm x 100 mm is centered 5 mm above the reference plane covering the trace.

The reference plane, with over the trace, is placed horizontally in the enclosure and is 10 mm away from the front panel and 10 mm above the bottom enclosure wall.

The trace is driven, with respect the reference plane, by a voltage signal whose waveform is depicted in Fig. 6. The voltage source and load terminations are of 50 ohm.

	DISCRETE PORT AS VOLTAGE SOURCE	
	DISCRETE PORT AS 50Ω LOAD	

Fig. 5 – Overview of the EM source; discrete port is used as a voltage source; discrete port is used as a 50Ω load.

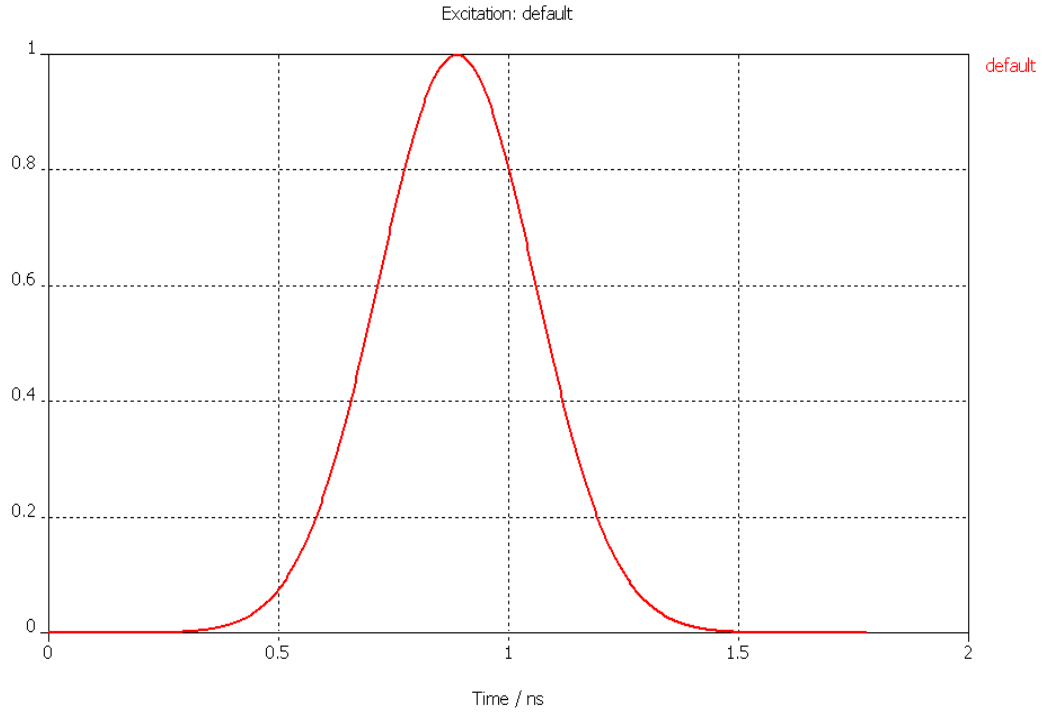


Fig. 6 – Excitation signal supplying the discrete port.

3.1 Enclosure with small holes

Considering the enclosure with small holes shown in Fig.2, it has been computed the magnitude of the electric field for two mesh settings: fine mesh and coarse mesh.

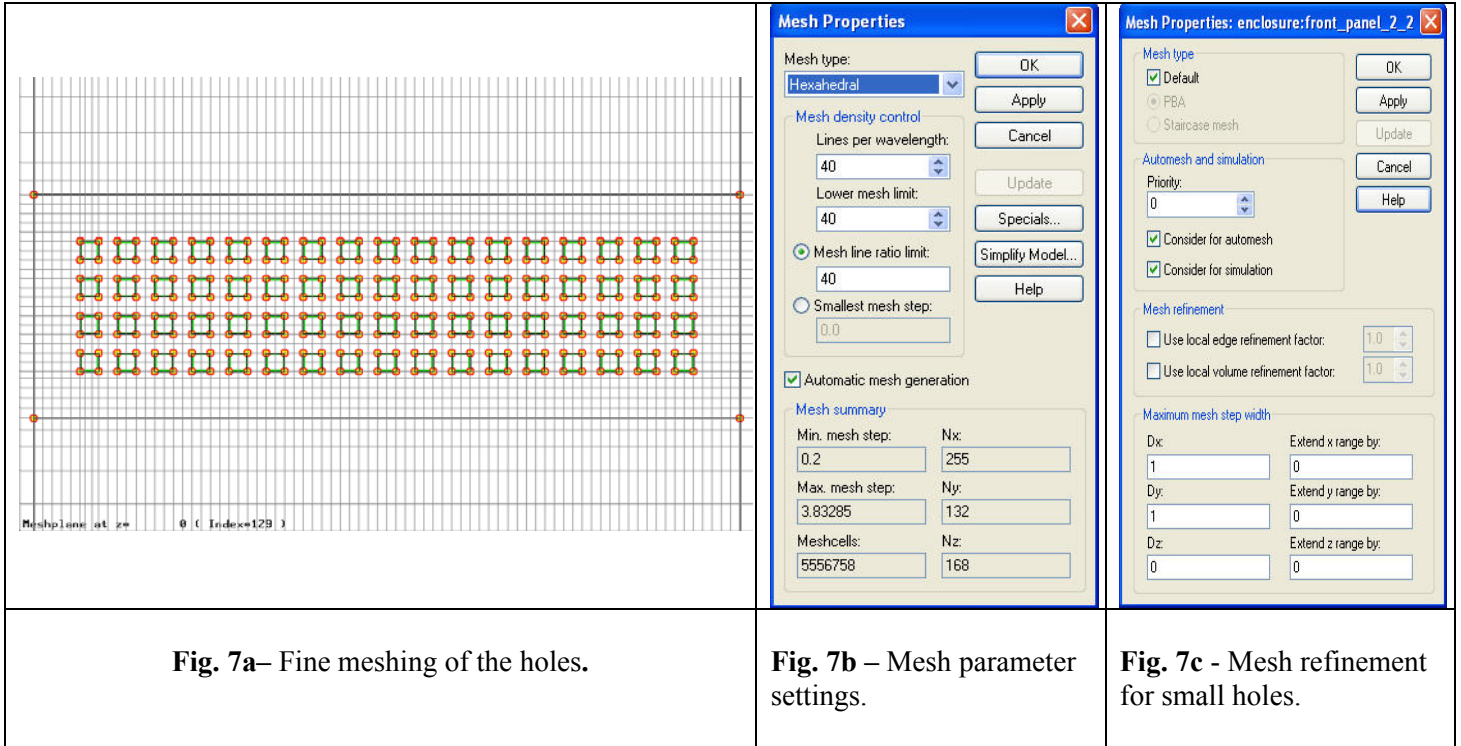
The magnitude of the electric field is computed as in (1):

$$E(f) = \sqrt{E_x^2(f) + E_y^2(f) + E_z^2(f)} \quad (1)$$

Where $E_x(f)$, $E_y(f)$ and $E_z(f)$ are the magnitude of the computed components of the electric field at distance of 3 m from the front side of the enclosure.

Fine mesh

The case with fine mesh is shown in Fig. 7a. The free space of the holes has been meshed with several lines in order to improve the reliability of the simulation. A summary of the basic settings is in Fig. 7b.



To add mesh line in holes', empty space a refined mesh is used whose settings are shown in Fig. 7c. For structure, elements of high importance for the simulation a maximum step width for every coordinate direction can be specified. The automatic mesh generator will not exceed this step width at the bounding box of this structure element.

Coarse mesh

The case with coarse mesh is shown in Fig. 8a and 8b. The mesh lines are placed in order to contour each holes without mesh lines in the free space of the holes. In Fig. 9 it is shown the comparison of the computed electric field magnitude for the case of fine and coarse mesh of the holes at a distance of 3 meter from the center of the front panel of the enclosure as depict in Fig. 10. Fig.11 shows the FSV comparison.

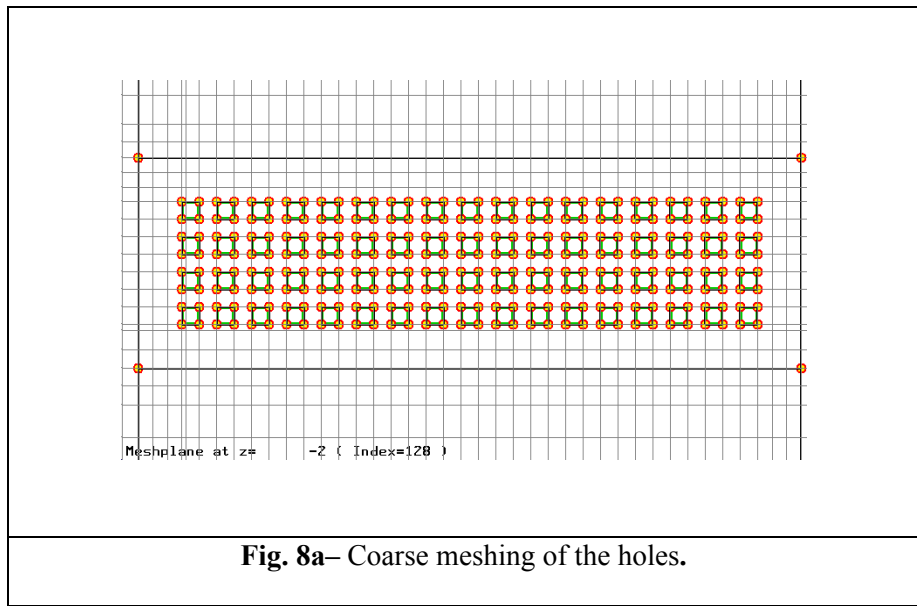


Fig. 8a– Coarse meshing of the holes.

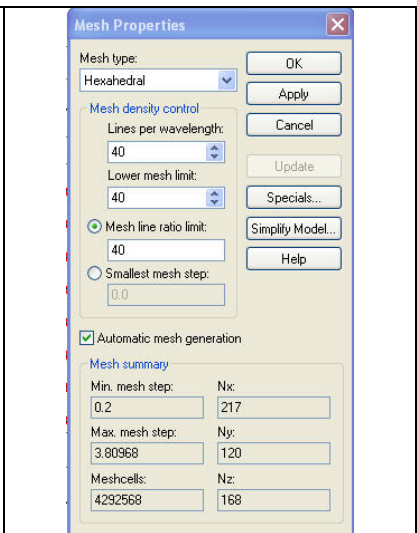


Fig. 8b – Mesh parameter settings.

Small holes: fine and coarse mesh results comparison

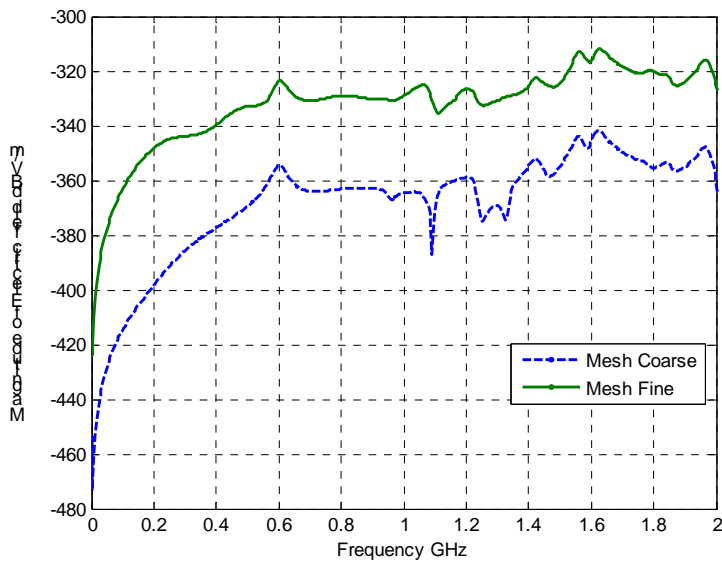


Fig. 9 – Small holes configuration: comparison the electric field magnitude at a distance of 3 m from the center of the front panel of the enclosure for coarse and fine mesh.



Fig. 10 – Electric field probe's distribution. Three probes are used each one of them for each component of the electric field.



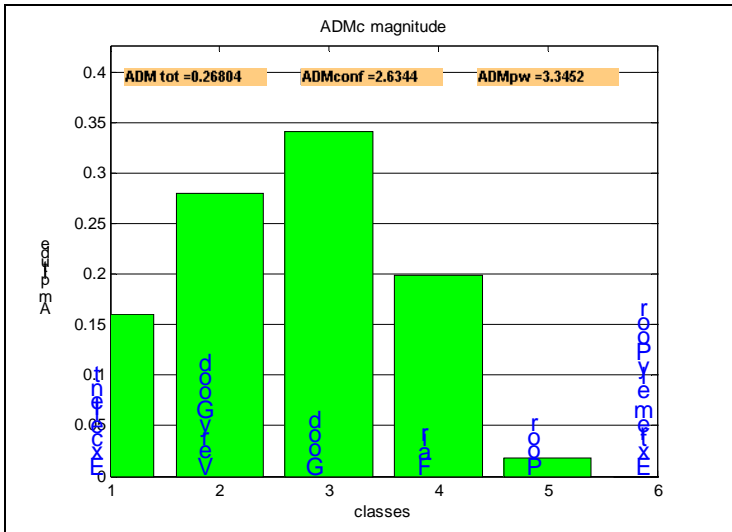


Fig. 11a – ADMc confidence histogram referred to Fig. 9.

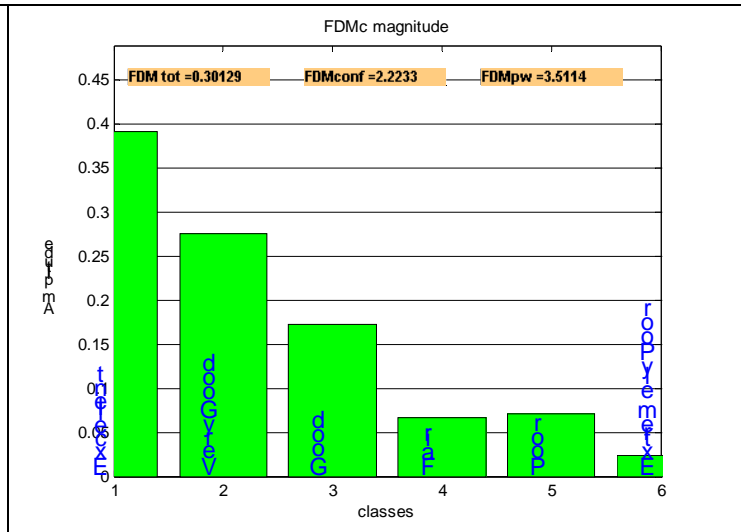


Fig. 11b - FDMc confidence histogram referred to Fig. 9.

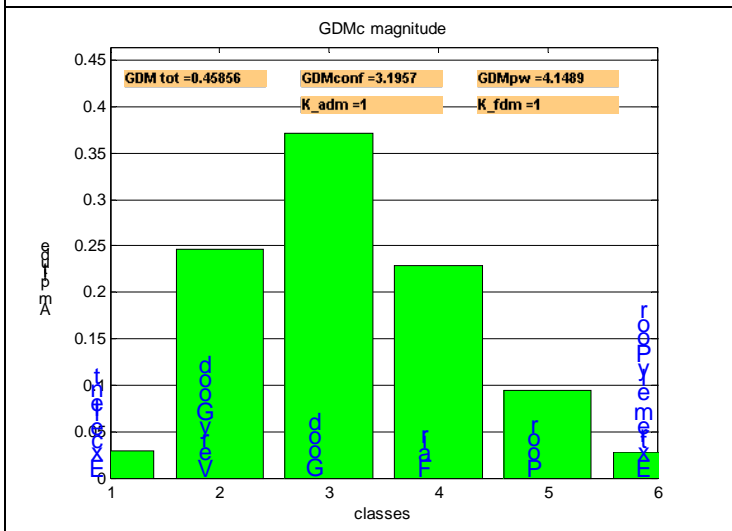


Fig.11c - GDMc confidence histogram referred to Fig. 9.

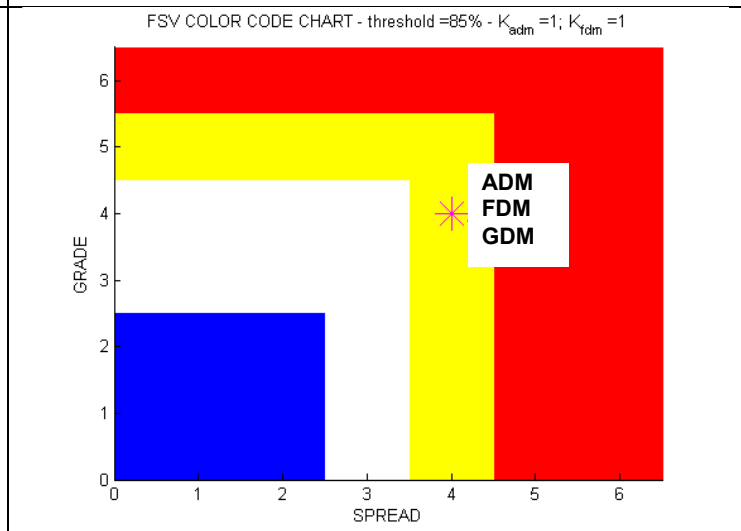


Fig. 11d – GRADE-SPREAD chart referred to Fig. 9.

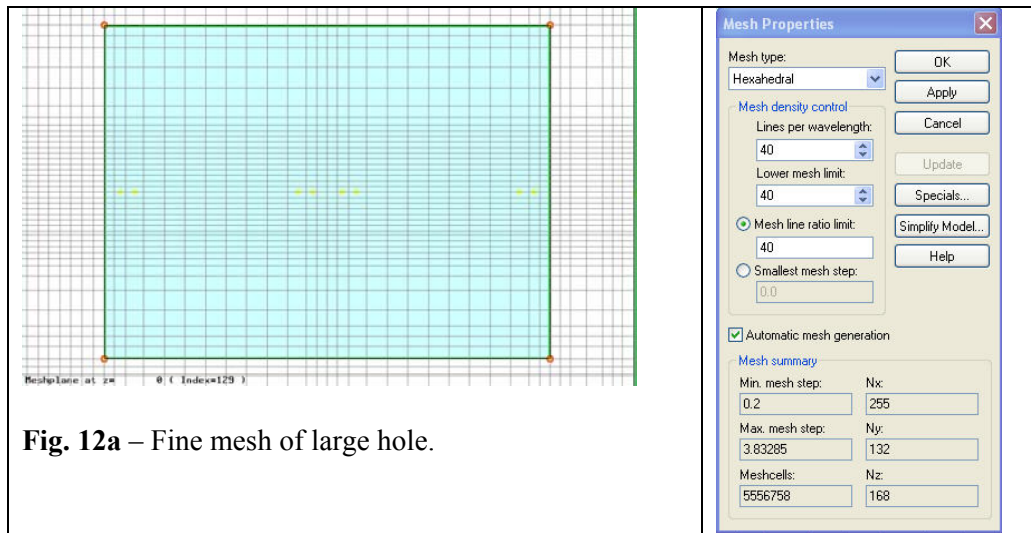
3.2 Enclosure with large hole

Considering the enclosure with large hole as depict in Fig. 3, it has been computed the magnitude of the electric field for two mesh settings: fine mesh and coarse mesh.

The magnitude of the electric field is always computed, as in (1).

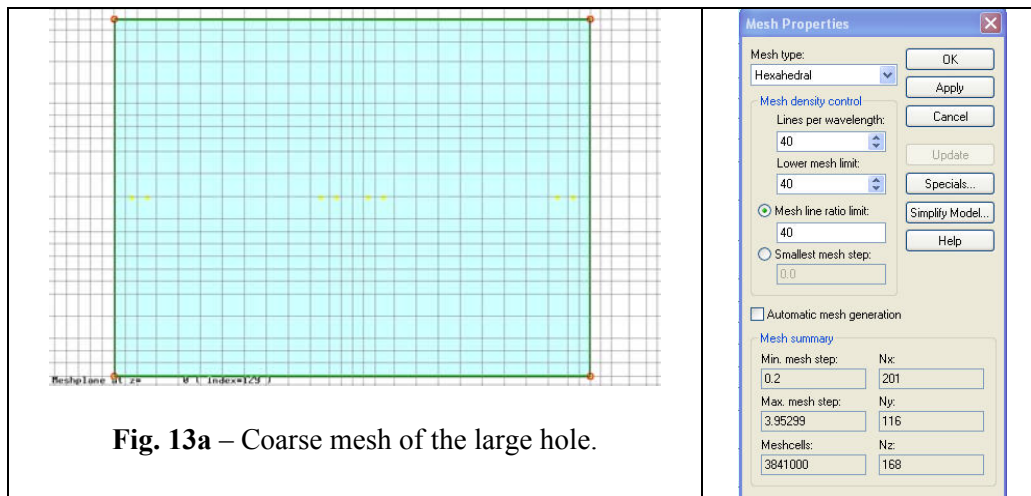
Fine mesh

The case with fine mesh is shown in Fig. 12. The free space of the large hole has been meshed with dense mesh lines. In Fig. 12b there is a summary of the mesh parameters.



Coarse mesh

The case with coarse mesh is shown in Fig. 13. The mesh lines are much less dense than those in Fig. 12a. Fig. 13b reports the corresponding settings.



Large hole: fine and coarse mesh results comparison

In Fig. 14, it is shown the comparison of the magnitude of the electric field computed for the case of fine and coarse mesh at a distance of 3 meters from the center of the front panel of the enclosure. In Fig. 14b, a zoom of the electric field magnitude from 1.4 GHz to 2 GHz is used to emphasize the difference between the compared curves. Fig. 15 shows the corresponding FSV comparison.

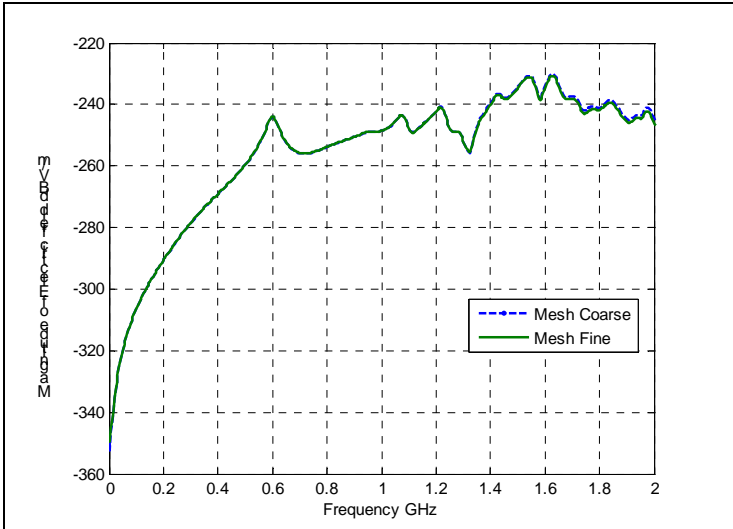


Fig.14a - Comparison the electric field magnitude at a distance of 3 m from the center of the front panel of the enclosure for coarse and fine mesh: large hole.

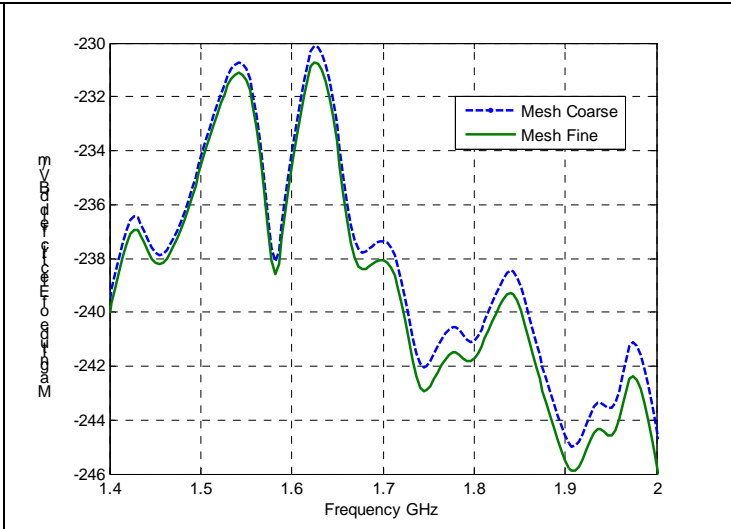


Fig. 14b – Comparison the electric field magnitude at a distance of 3 m from the center of the front panel of the enclosure for coarse and fine mesh; zoom in frequency range from 1.6 GHz to 2 GHz: large hole.

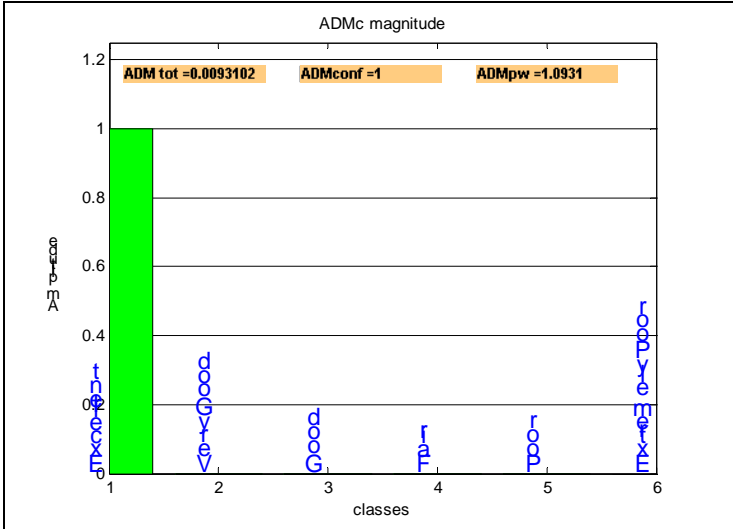


Fig. 15a - ADMc confidence histogram referred to Fig. 14a.

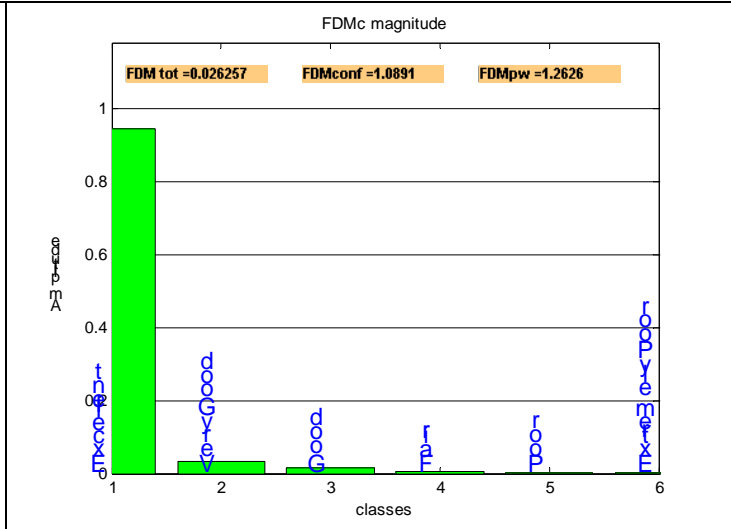


Fig. 15b - FDMc confidence histogram referred to Fig. 14a.

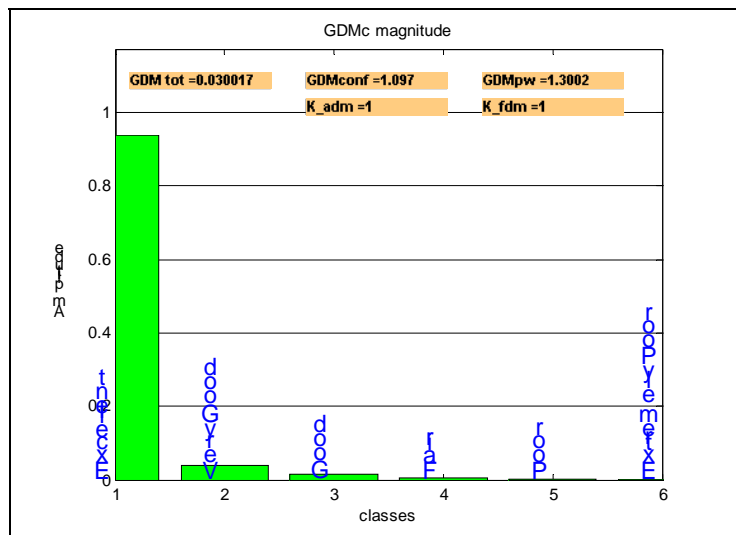


Fig. 15c - GDMc confidence histogram referred to Fig. 14a.

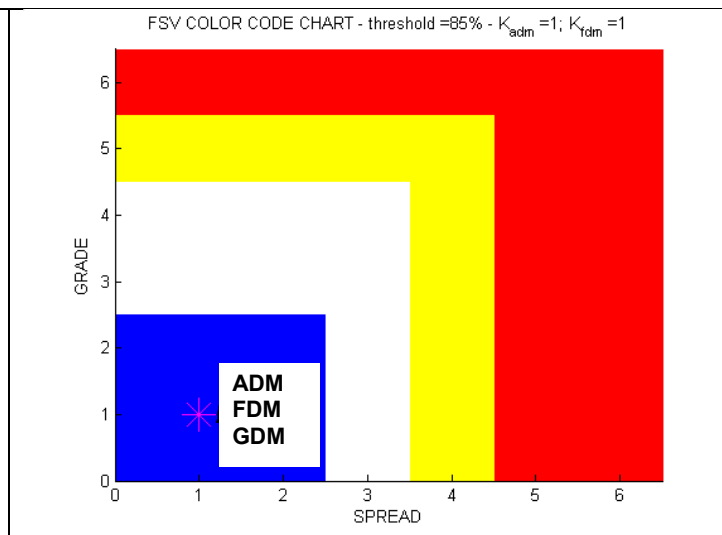


Fig. 15d - GRADE-SPREAD chart referred to Fig. 14a.

3.3 Remarks

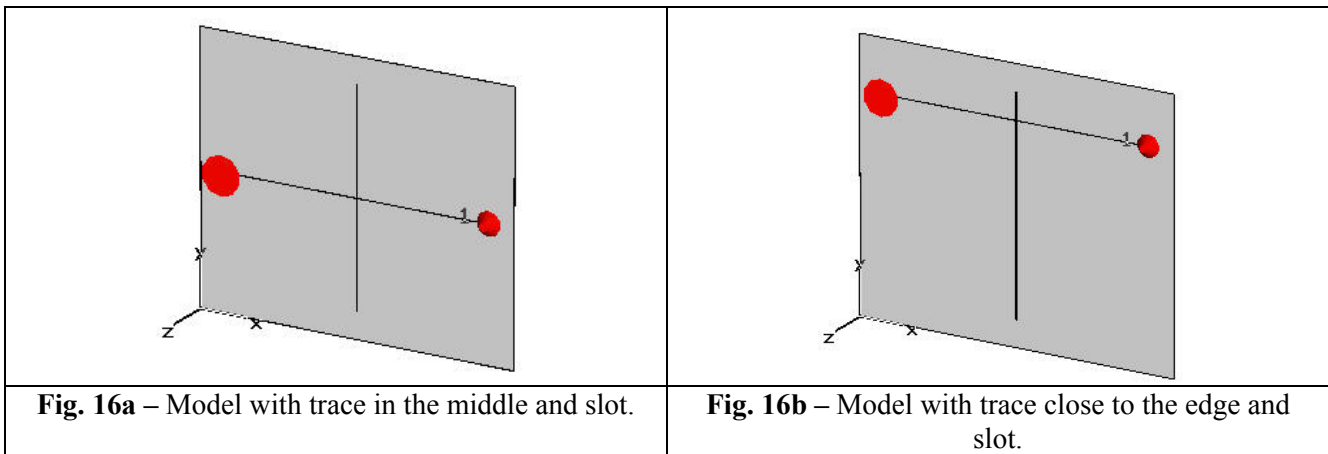
The results in terms of magnitude of the electric field computed 3 meters distant from the front side of the enclosure are different for the different mesh setting parameters used considering small holes or large hole.

In the case of small holes the comparison of the results due to different mesh setting shows the curves have the same shape but are different in the details. The difference is about 30 dB and is uniform along the considered frequency range.

4. A PCB STANDARD PROBLEM

The emissions from a PC board where a trace is run over a split in the ground-reference plane is due to a complex interaction of the return current ‘loop’ in the ground-reference plane, and the extra ‘bunching’ of return current near the edge of the ground-reference plane. These effects result in an increase of radiated emissions, and a negative EMI impact.

The aim of this section is to compute and compare the maximum of the electric field over a spherical surface 3 m away from the center of the PCB for different simulations mesh settings. The board with slot on reference plane and trace in the middle of the substrate and the board with slot in the reference plane and the trace over the substrate close to the board edge, as shown in Fig.16, have been investigated. For both cases, different mesh settings for the slot have been used and then the comparison of the results of varying the mesh are shown. The detailed description of the whole system follows in the next section.

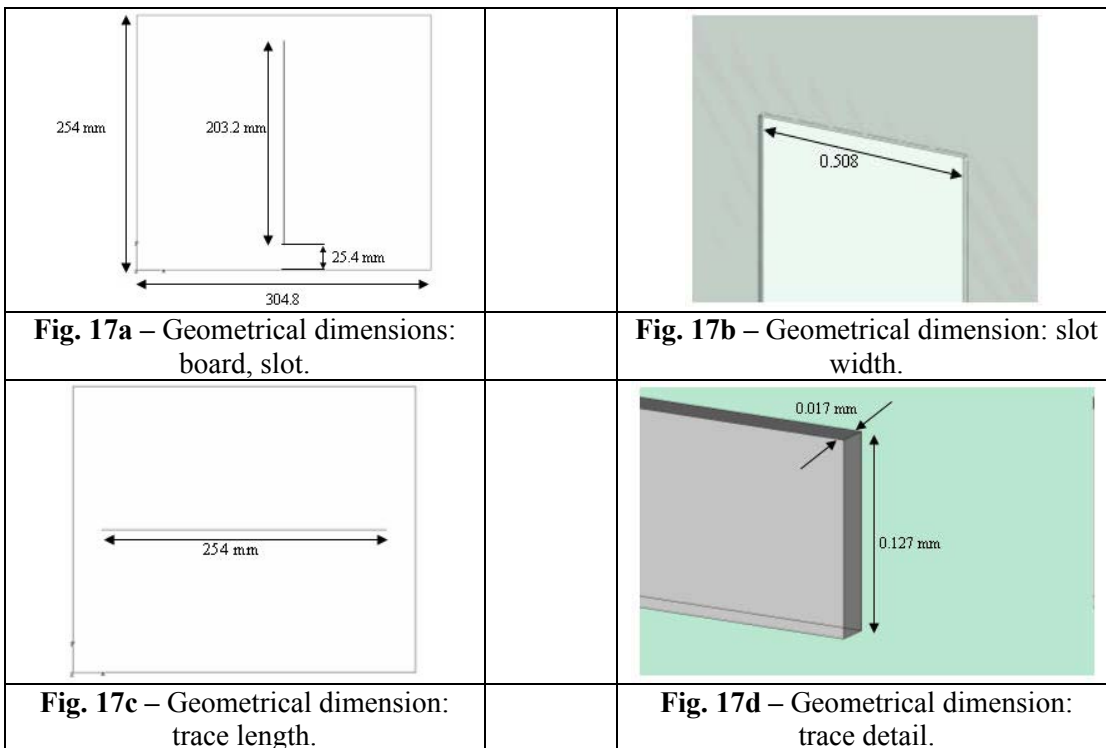


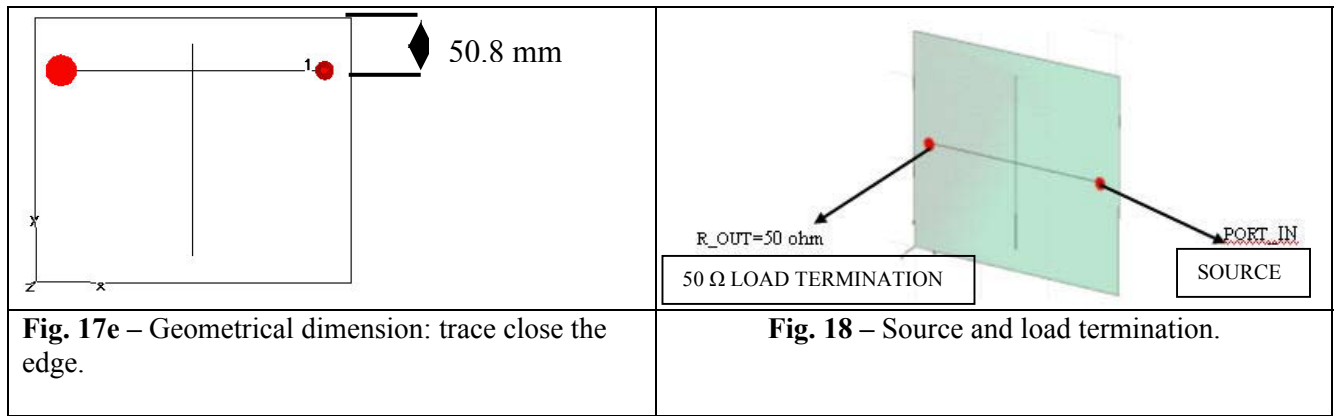
The geometrical dimensions of the entire structure are shown in Fig. 17. The analysis has been performed in the frequency range 0.1GHz - 2GHz.

PCB Dimensions and materials (see Fig. 17):

The PCB is simulated as follows: there is a metal plane (*Reference Plane*) in PEC material with dimensions 304.8 mm x 254 mm x 0.017 mm (x, y, z axis). Over the metal plane there is a dielectric substrate of FR4 whose dimensions are 304.8 mm x 254 mm x 0.127 mm; its dielectric permittivity is $\epsilon_r = 4.7$ and no dielectric losses are considered. The trace in PEC material is placed over the dielectric substrate (microstrip configuration); the trace has dimensions of 254 mm x 0.127 mm x 0.017 mm and is considered in two different positions: centered or close to the upper edge respectively (see Fig.16a and Fig. 16b).

The slot is centered in the reference plane and its dimensions are 0.508 mm x 203.2mm.





Source / load termination (see Fig. 18):

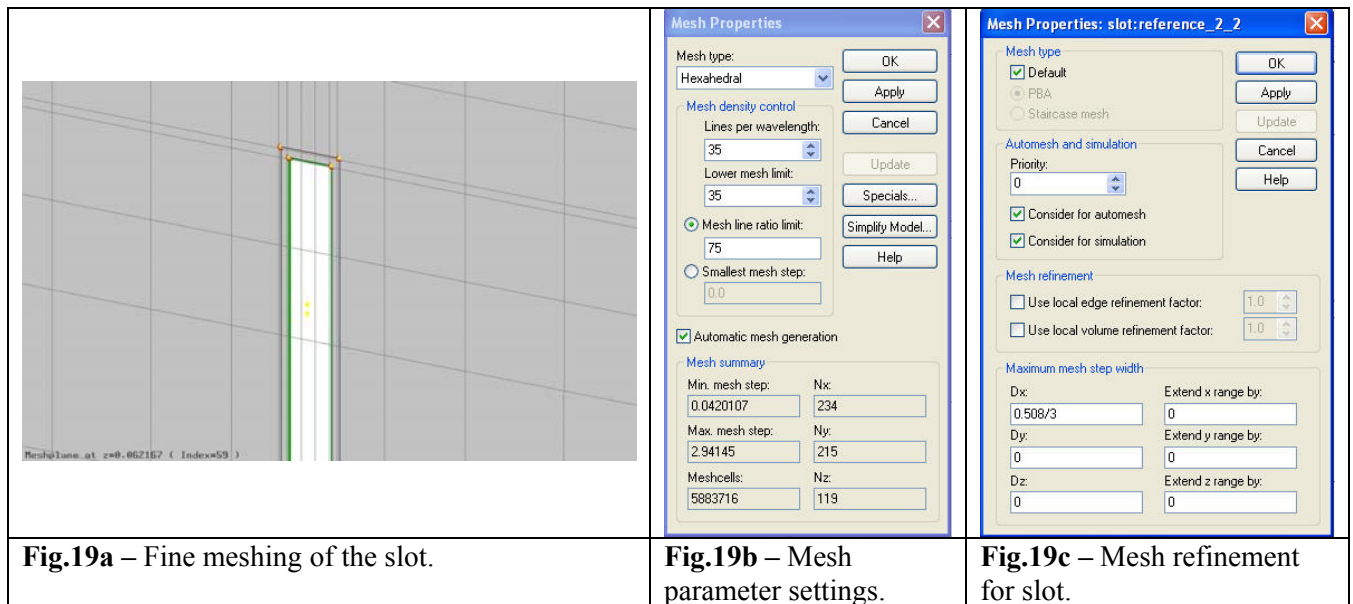
The metal plane (representing the PCB reference plane) and the trace over a dielectric are driven by a 3.3 V voltage source in the above mentioned frequency range. The source and load terminations are of 50 Ω as in Fig. 18.

4.1 Board with slot, trace in the middle

Considering the board with slot on reference plane and trace in the middle, it has been computed the maximum electric field over a spherical surface 3 m away from the center of the PCB for two mesh settings of the slot: fine mesh and coarse mesh.

Fine mesh

The case with fine mesh is shown in Fig. 19 in which are also reported the mesh properties. The free space of the slot has been meshed with several mesh lines.



Coarse mesh

The case with coarse mesh is shown in Fig 20. The mesh line is placed in order to contour the slot without any mesh lines in the free space of the slot.

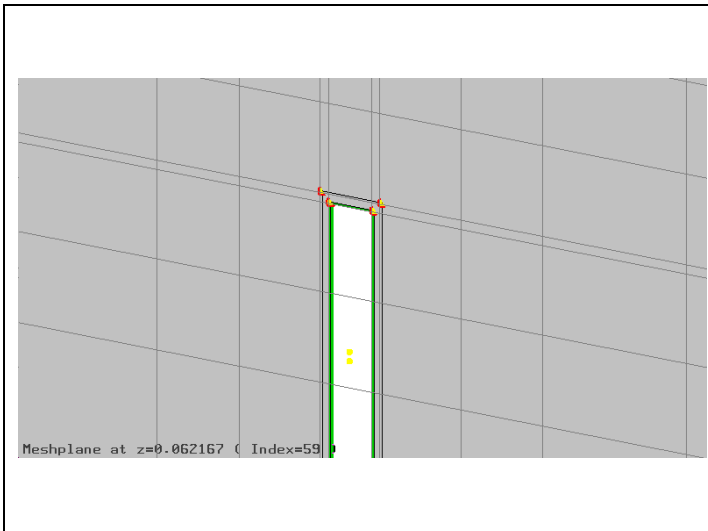


Fig. 20a – Coarse meshing of the slot.

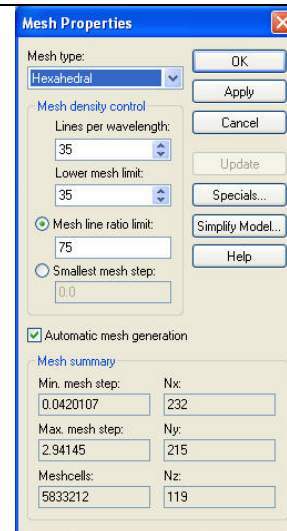


Fig. 20b – Mesh parameter settings.

Board with slot, trace in the middle: fine and coarse mesh results comparison

In Fig. 21 is shown the comparison, for slot's fine and coarse mesh, of the maximum electric field computed over a spherical surface at a distance of 3 meter from the center of the PCB for the case board with slot, trace in the middle. Fig. 22 shows the FSV comparison.

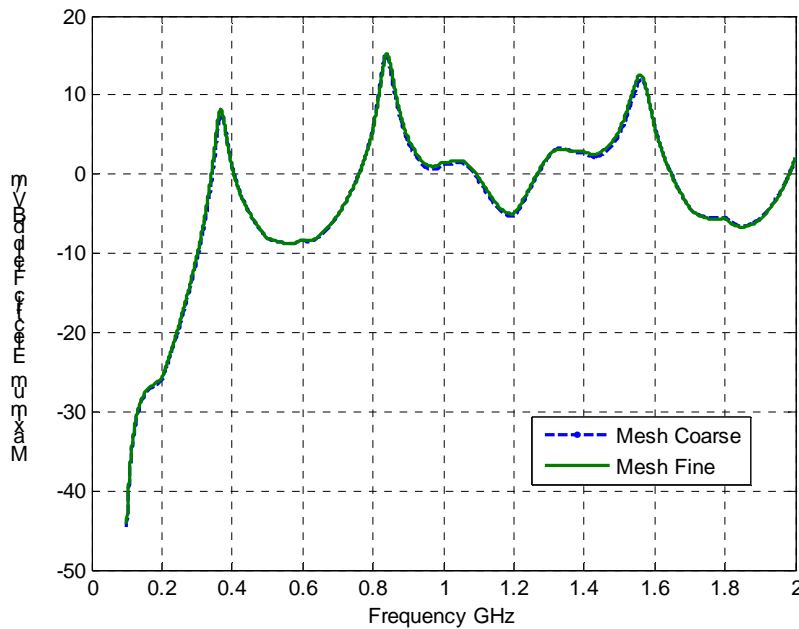


Fig. 21 – Comparison of the maximum electric field computed over a spherical surface at a distance of 3 meter from the center of the PCB: board with slot trace in the middle, fine and coarse mesh.

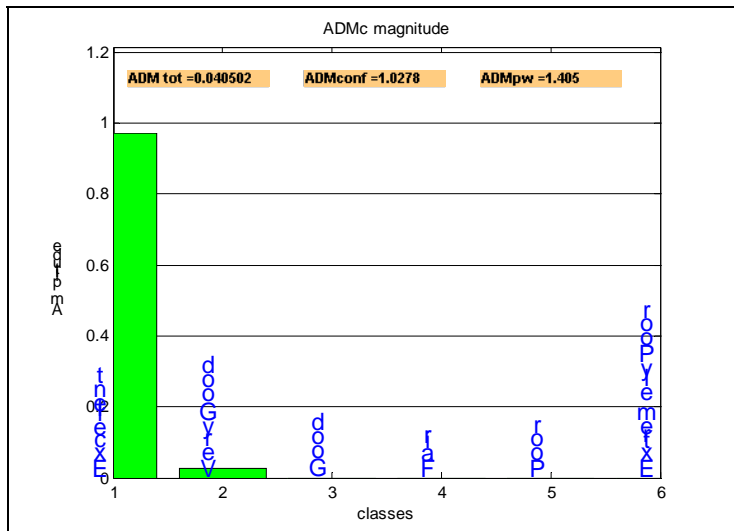


Fig. 22a - ADMc confidence histogram referred to Fig. 21.

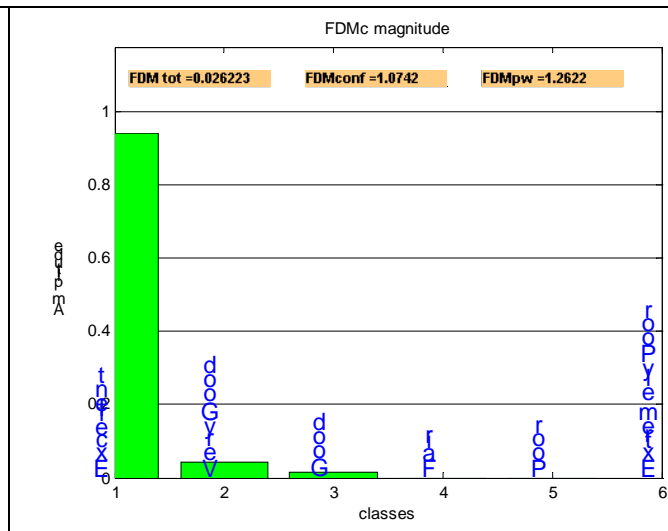


Fig. 22b - FDMc confidence histogram referred to Fig. 21.

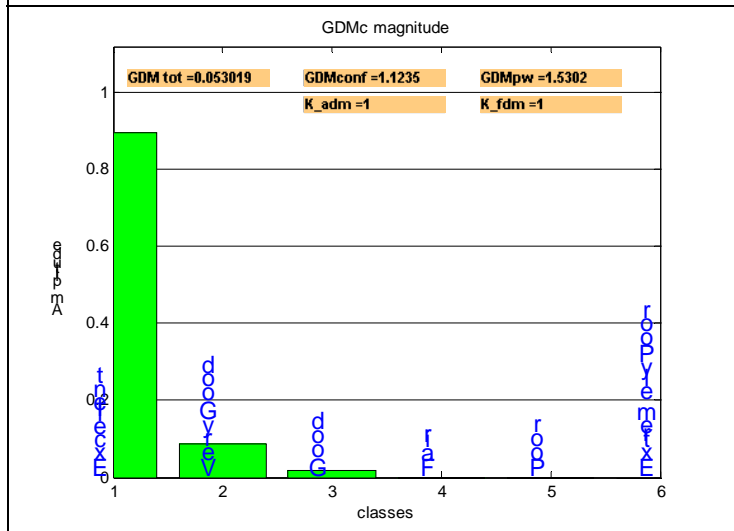


Fig. 22c - GDMc confidence histogram referred to Fig. 21.

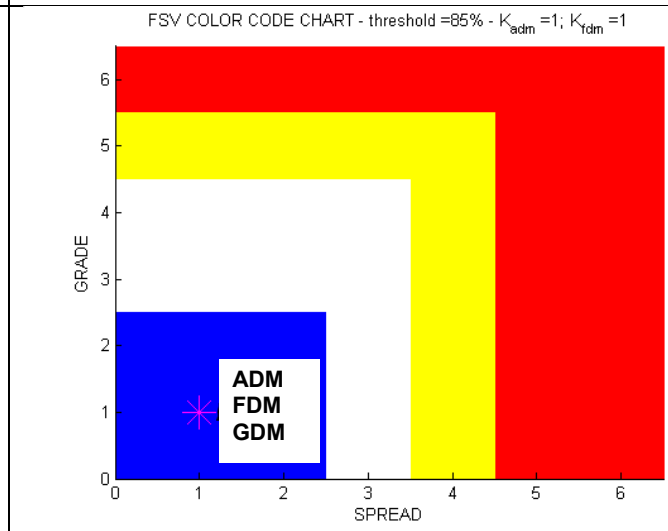


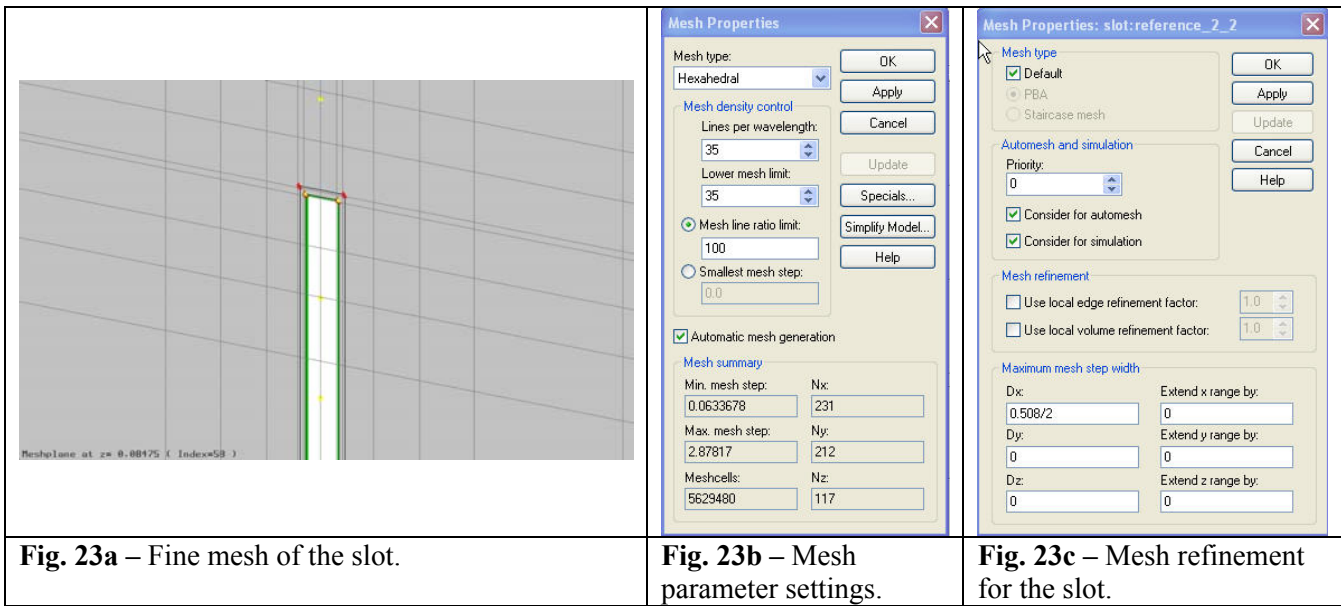
Fig. 22d - GRADE-SPREAD chart referred to Fig. 21.

4.2 Board with slot, trace close to the board edge

Considering the board with slot on reference plane and trace close to the board edge of the substrate, it has been computed the maximum electric field over a spherical surface 3 m away from the center of the PCB for two mesh settings of the slot: fine mesh and coarse mesh.

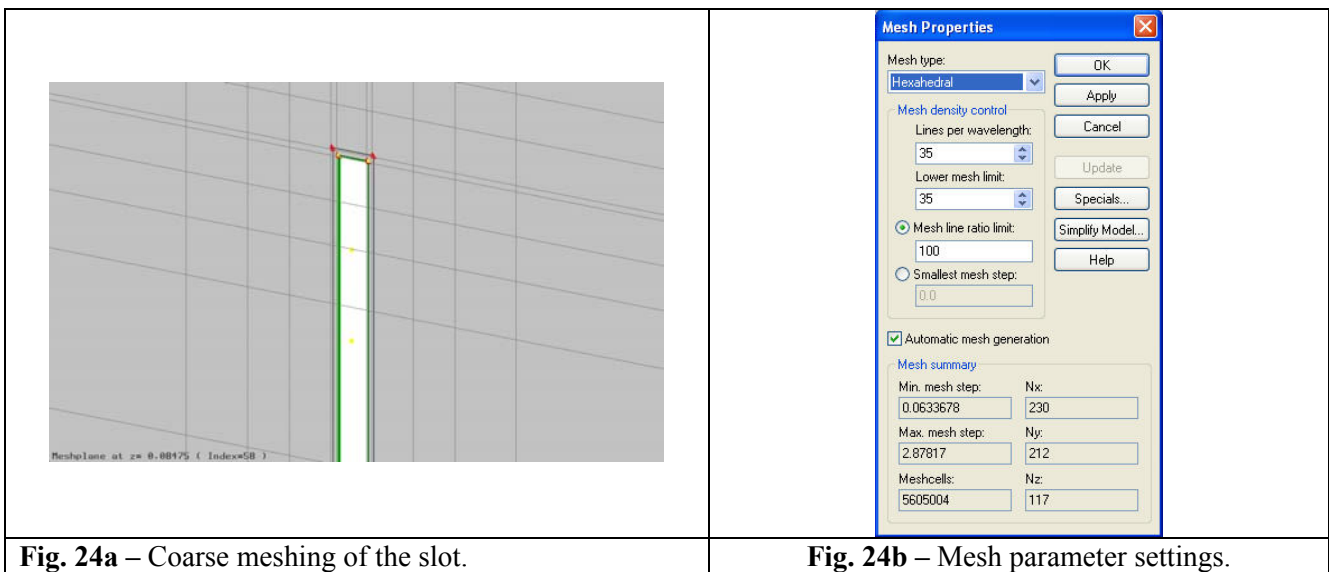
Fine mesh

For the case with fine mesh, (see Fig. 23a), the parameters of the mesh settings are as in Fig. 23b and 23c. The free space of the slot it has been filled with several mesh lines.



Coarse mesh

The parameters settings for the case with coarse mesh are shown in Fig. 24 along with the meshed slot. The mesh lines are placed in order to contour the slot without any vertical line in the free space of the slot.



Board with slot, trace close to the edge: fine and coarse mesh results comparison

In Fig. 25 is shown the comparison, for slot's fine and coarse mesh, of the maximum electric field computed over a spherical surface at a distance of 3 meter from the center of the PCB for the case board with slot, trace close to the board edge. Fig. 26 shows the FSV comparison.

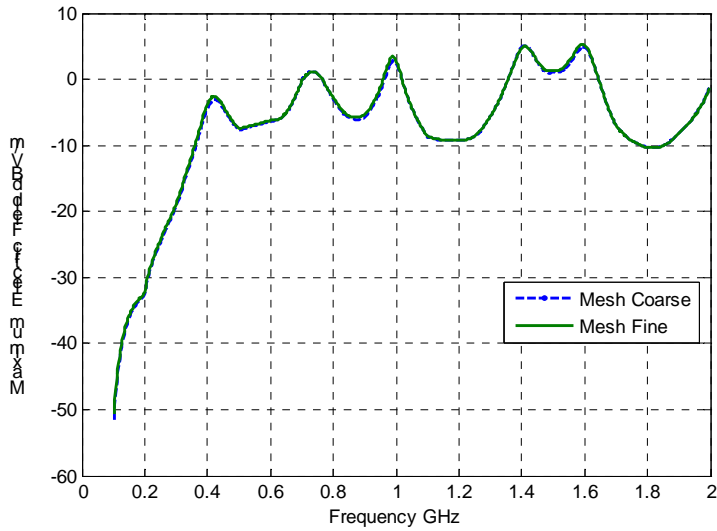


Fig. 25 – Comparison of the maximum electric field computed over a spherical surface at a distance of 3 meters from the center of the PCB: board with slot, trace close to the board edge.

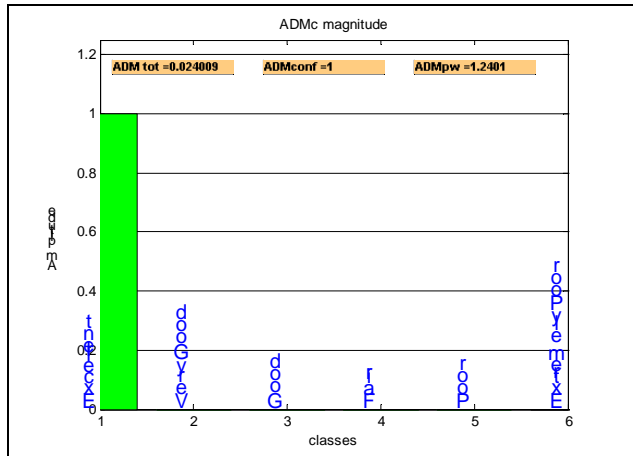


Fig. 26a – ADMc confidence diagram referred to Fig. 25.

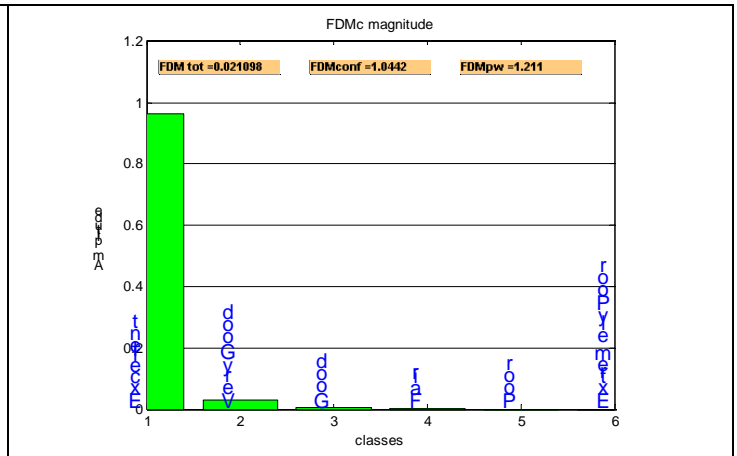


Fig. 26b - FDMc confidence diagram referred to Fig. 25.

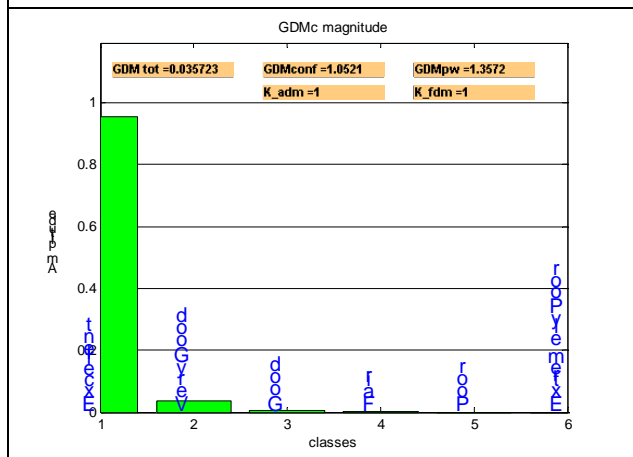


Fig. 26c - GDMc confidence diagram referred to Fig. 25.

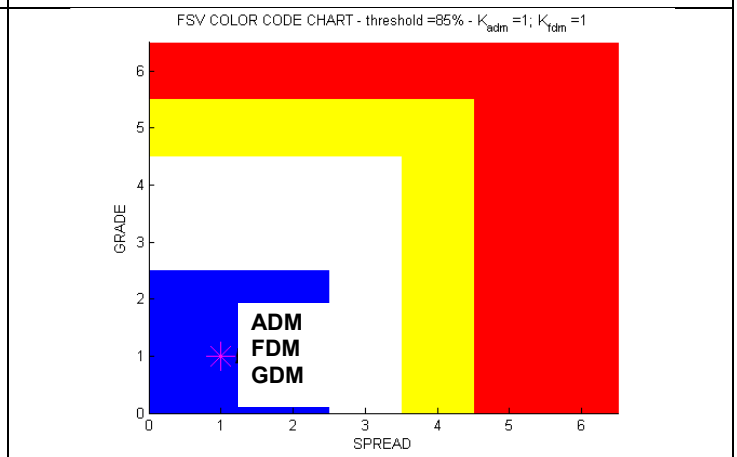


Fig. 26d – GRADE-SPREAD chart referred to Fig. 25.

4.3 Remarks

The comparison of the maximum electric field computed over a spherical surface at a distance of 3 meters from the center of the PCB between models with fine and coarse mesh either for the case with trace in the middle and trace close to the board edge is in good agreement. The slot meshing on reference plane has a little impact on the computed results.

5. A SIGNAL INTEGRITY STANDARD PROBLEM

This model concerns the performance of a delay line on a printed circuit board. Signal traces are often created in various serpentine shapes to lengthen the trace length and achieve a desired delay. The coupling between the legs of the serpentine delay line can create significant distortion in the pulse, which is not simulated in typical transmission line based simulation tools. The distortion can easily cause timing problems as well as create common mode currents, which can cause, in turn, EMC problems.

In this chapter, it has been investigated the electromagnetic behavior of a board on which a meander delay or an equivalent length straight line is printed. For the first case, the aim is to compute the transient voltage waveform across the load termination depending on the simulations mesh settings. It has been analyzed the impact of the meander meshing on the computed results. For the second case it has been analyzed the impact of the GND plane extension on the transient voltage waveform across the load termination and the impact of the dielectric meshing. A detailed description of the systems is explained below.

Two different configurations it has been considered. The first one is a model of a board on which a meander delay line is printed: Fig. 27 shows the geometry for this model. The second one is the model of a board on which a straight line is printed whose length is equal to that of the meander line. This is referred as equivalent length straight line and its geometry is shown in Fig. 28. For both configurations, the source is a voltage pulse of trapezoidal shape as shown in Fig. 29. For both configurations it has been computed the transient voltage waveform across the load termination.

PCB Dimensions and Materials:

Meander Delay Line Model (see Fig. 27) - The PCB model has the following characteristics: the reference plane is in Perfect Electric Conductor (PEC) material whose dimensions are 23.25 mm \times 40.25 mm \times 0.2 mm (x,y,z axis). On the PEC plane there is a dielectric substrate of FR4 whose dimensions are 23.25 mm \times 40.25 mm \times 0.25 mm; its relative dielectric permittivity is $\epsilon_r = 4.5$ and no dielectric losses are considered. The meander trace, in PEC materials, is placed on the dielectric substrate and, like a serpentine, has a number of closely coupled legs. The trace has the following dimensions : 0.25mm wide; 0.2mm thick; 0.25mm legs separation. The trace is simulated as a PEC material. The exact characteristic impedance of the line is 56 Ω .

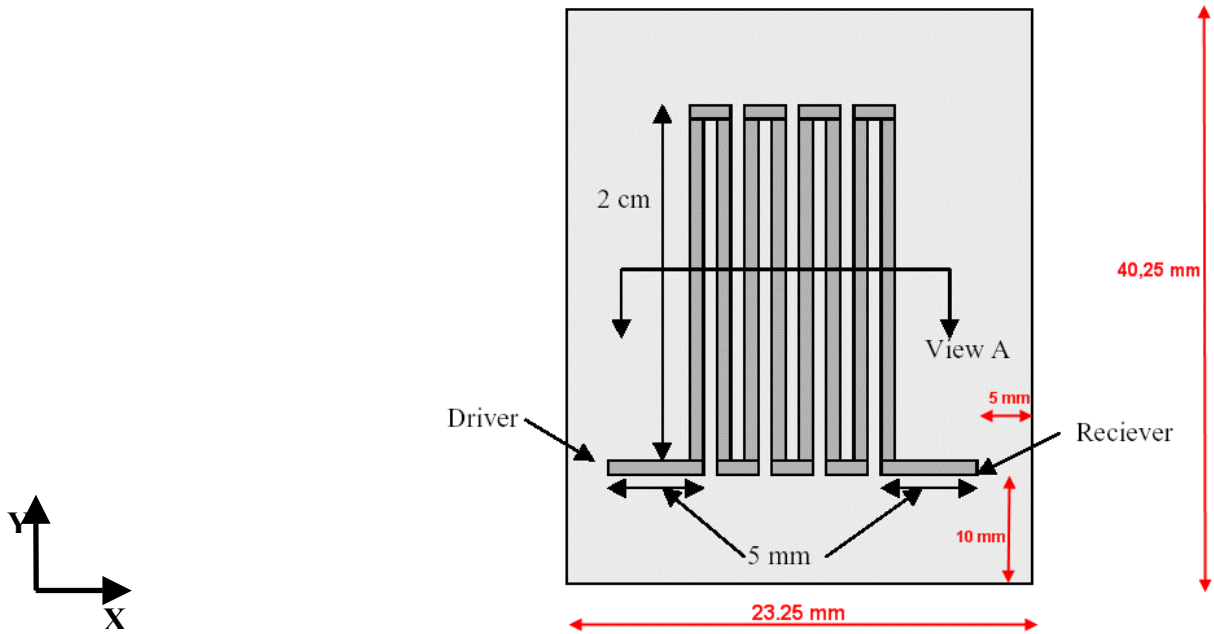


Fig. 27a - Meander delay line (Top View).

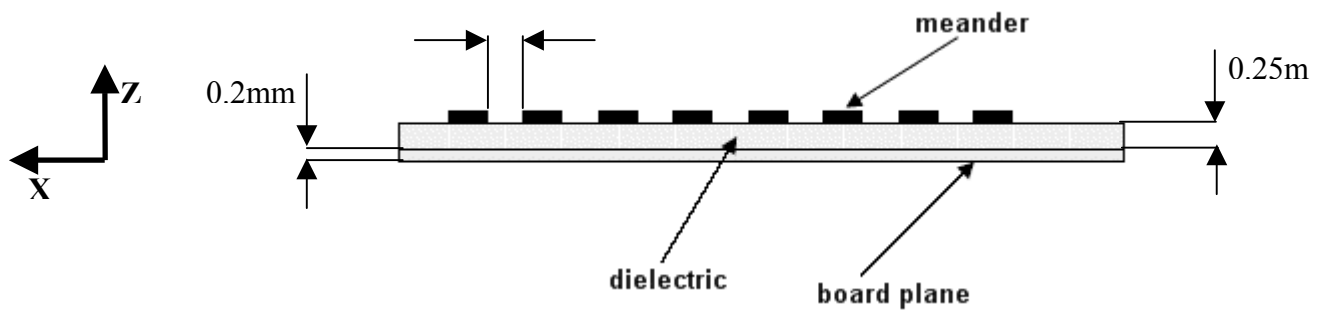


Fig. 27b - Meander delay line cross section (View A).

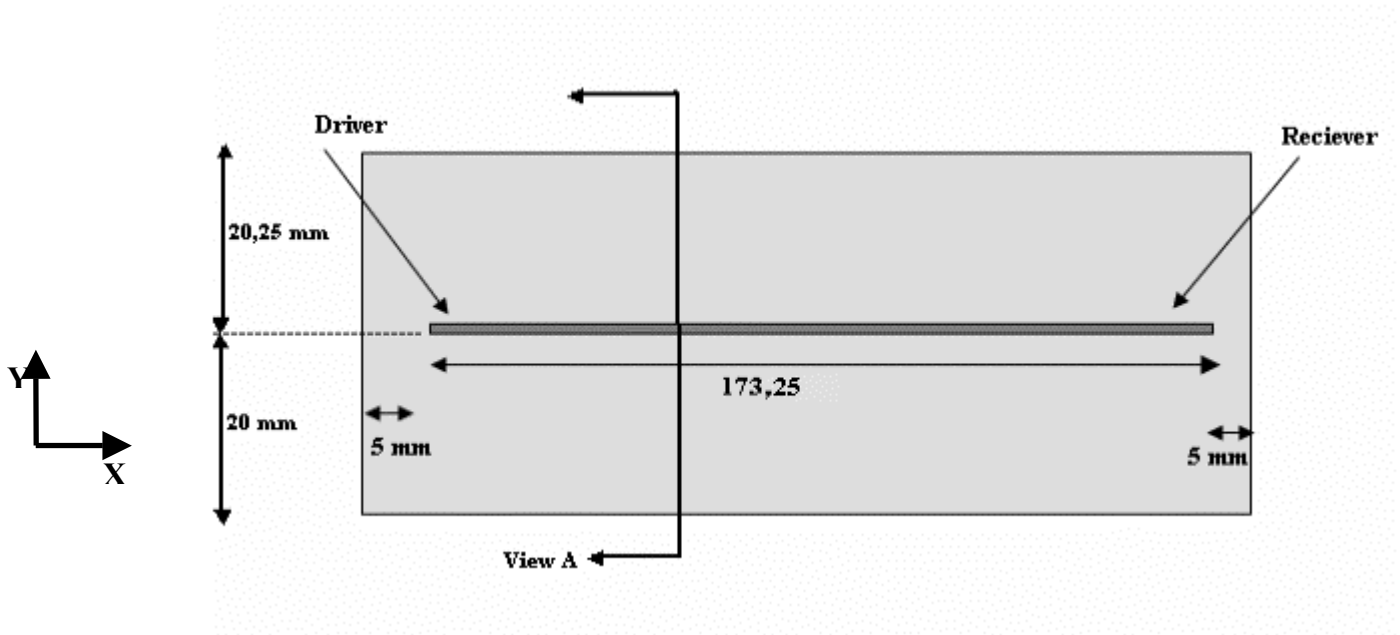


Fig. 28a – Equivalent length straight line.

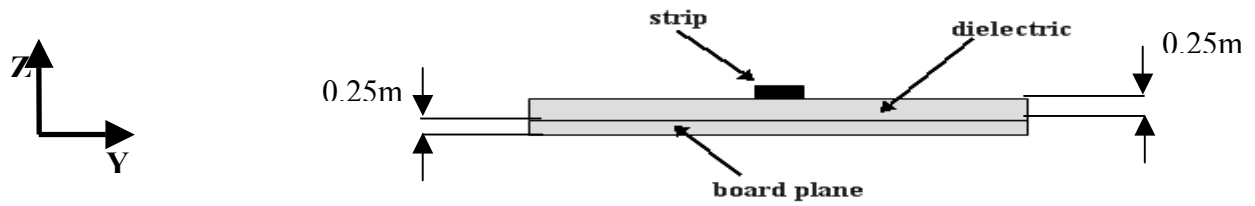


Fig. 28b – Equivalent length straight line cross section (View A).

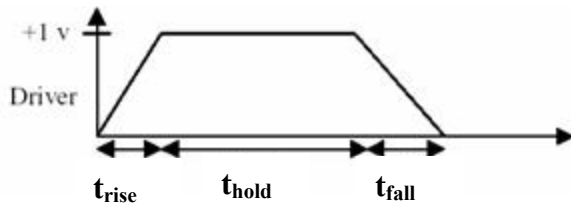


Fig. 29a – Excitation pulse;
 $t_{\text{rise}}=0.2\text{ns}$, $t_{\text{fall}}=0.2\text{ns}$, $t_{\text{hold}}=1\text{ns}$.



Fig. 29b – Excitation pulse,
 Microwave studio settings.

Equivalent Length Straight Line Model (see Fig. 28) - The PCB model has the following characteristics: the reference plane is in Perfect Electric Conductor (PEC) material whose dimensions are 183.25 mm x 40.25 mm x 0.2 mm (x,y,z axis). On the PEC plane there is a dielectric substrate of FR4 whose dimensions are 183.5 mm x 40.25 mm x 0.25 mm; its dielectric permittivity is $\epsilon_r = 4.5$ and no dielectric losses are considered. The straight trace in PEC materials is placed on the dielectric substrate. The trace is simulated as a PEC material. The characteristic impedance of the line is 50 Ω .

Source / Load Termination:

Meander Delay Line Model – The trace is driven against the reference plane by a trapezoidal voltage pulse of amplitude equal to 1V amplitude, $t_{\text{rise}}=0.2\text{ns}$, $t_{\text{fall}}=0.2\text{ns}$, and $t_{\text{hold}}=1\text{ns}$, as shown in Fig. 29. The length of the considered time window is 10ns. The load termination is a resistive impedance equal to the characteristic impedance of the line $Z_{\text{load}} = 56\Omega$; the internal impedance of the voltage source is set $Z_{\text{source}} = 0\Omega$. The structure it has been excited with a voltage discrete port [4].

Equivalent Length Straight Line Model - The trace is driven against the reference plane by a trapezoidal voltage pulse of amplitude equal to 1V amplitude, $t_{\text{rise}}=0.2\text{ns}$, $t_{\text{fall}}=0.2\text{ns}$, and $t_{\text{hold}}=1\text{ns}$, as shown in Fig. 29. The length of the considered time window is 10ns. The load termination is a resistive impedance equal to the characteristic impedance of the line $Z_{\text{load}}= 50\Omega$; the internal impedance of the voltage source set $Z_{\text{source}} = 0\Omega$. The structure it has been excited with a voltage discrete port [4].

5.1 Board with printed meander delay line

Considering the board with meander delay line it has been computed the transient voltage waveform across the load termination for two mesh settings of the empty space between meander legs: fine mesh and coarse mesh.

5.1.2 Fine mesh

The case with fine mesh is shown in Fig. 30. The free space between legs has been meshed with dense mesh lines.

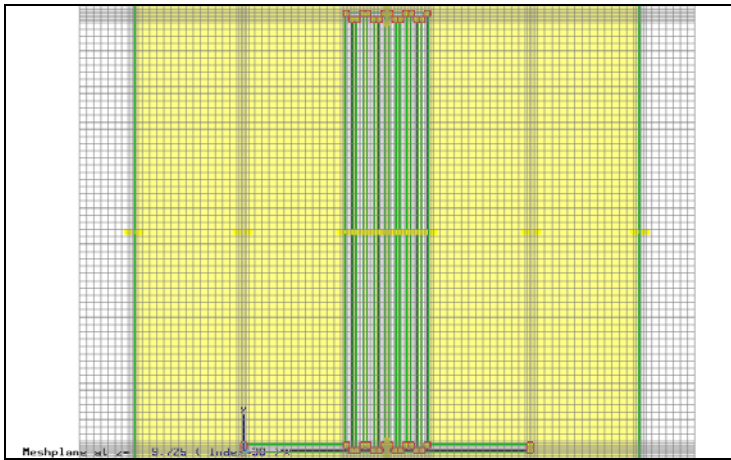


Fig. 30a – Fine meshing of the space between legs.

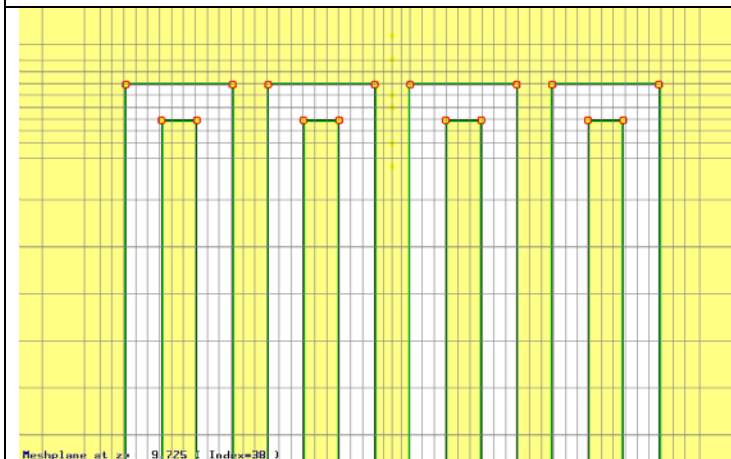


Fig. 30b – Zoom of the mesh between leg's space.

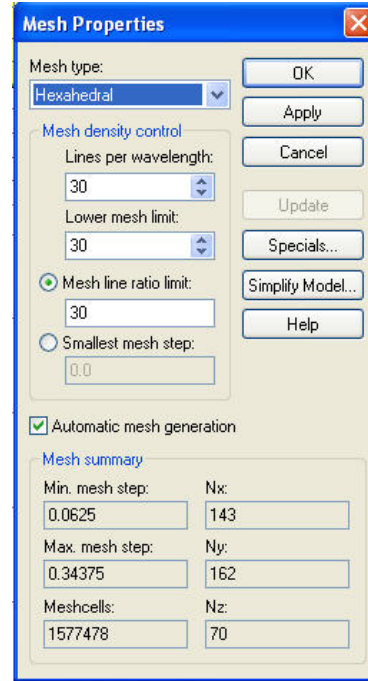


Fig. 30c – Mesh parameter settings.

5.1.3 Coarse mesh

The case with coarse mesh is shown in Fig 31. The mesh line is placed in order to contour the legs without vertical mesh lines between them.

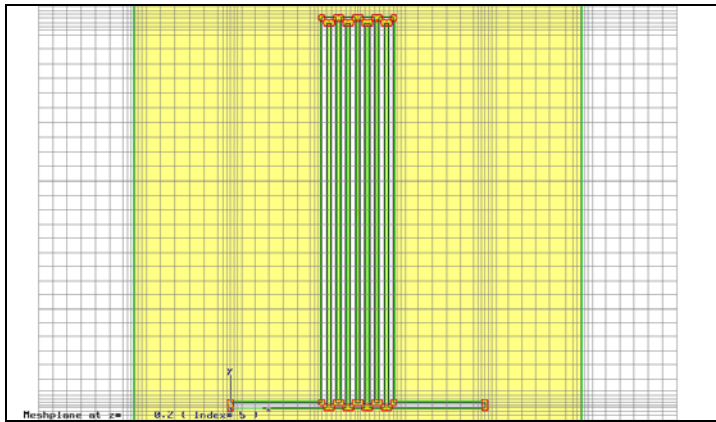


Fig. 31a – Coarse meshing of the space between legs.

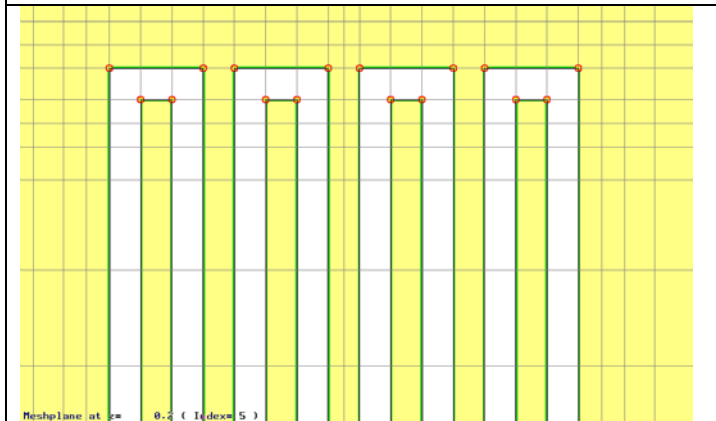


Fig. 31b – Zoom of the mesh between legs space.

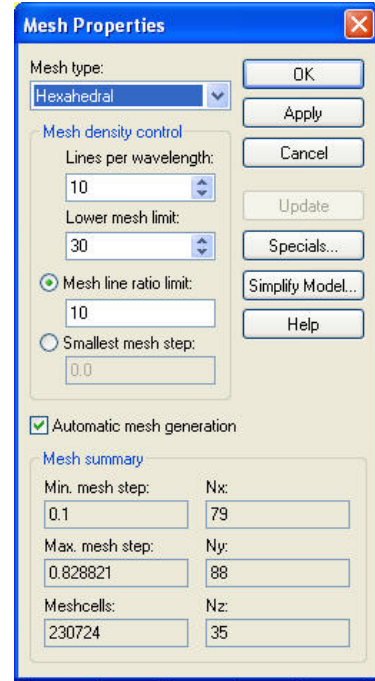


Fig. 31c – Mesh parameter settings.

Board with printed meander delay line: fine and coarse mesh results comparison

In Fig. 32 is shown the comparison, for fine and coarse mesh, of the transient voltage waveform across the load termination for the case board with printed meander delay line. Fig. 33 shown the FSV comparison.

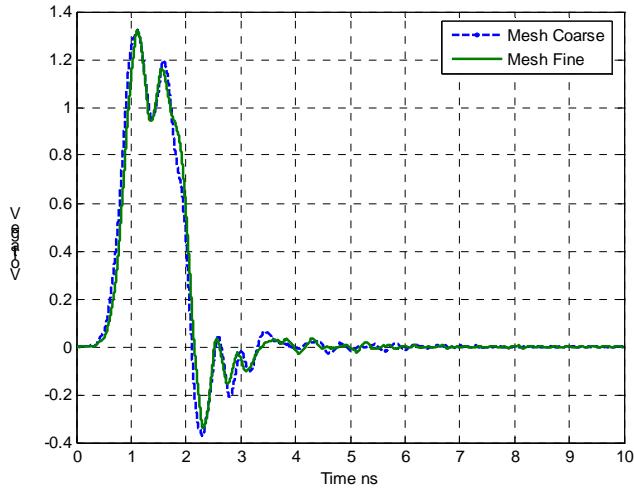


Fig. 32 – Comparison of the transient voltage waveform across the load termination: board with printed meander delay line.

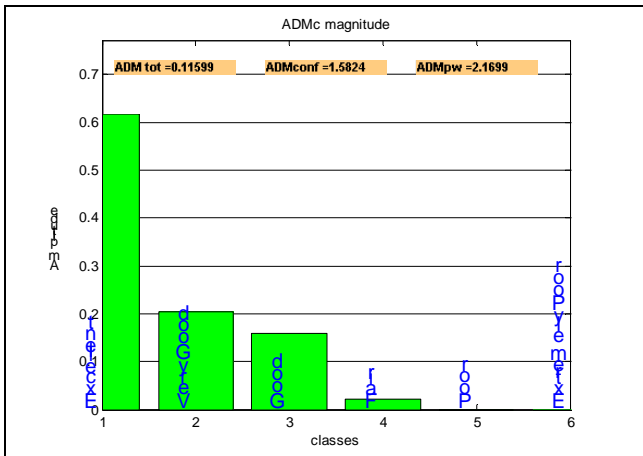


Fig. 33a - ADMc confidence diagram referred to Fig. 32.

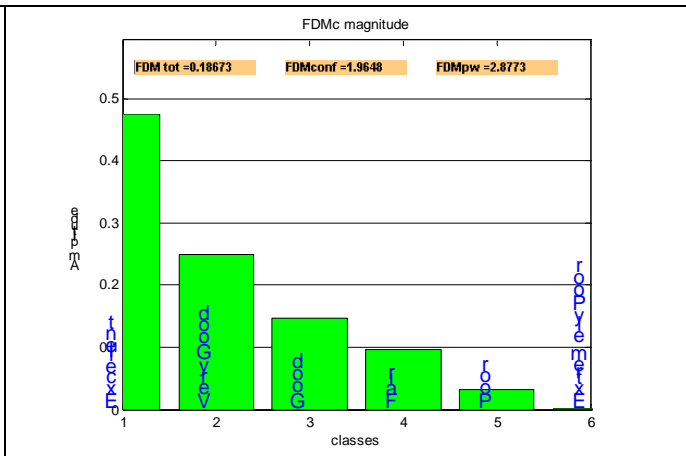


Fig. 33b - FDMc confidence diagram referred to Fig. 32.

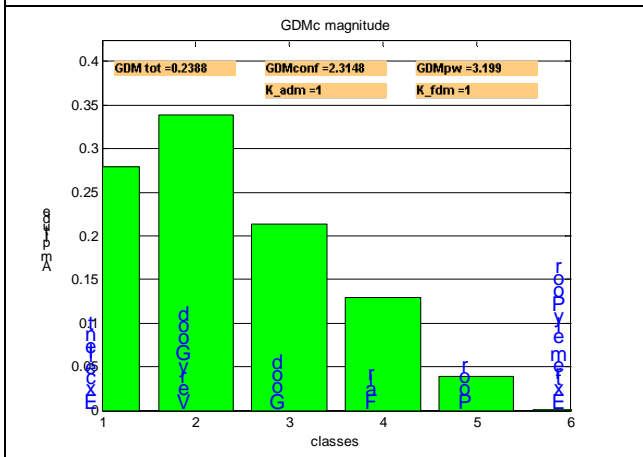


Fig. 33c - GDMc confidence diagram referred to

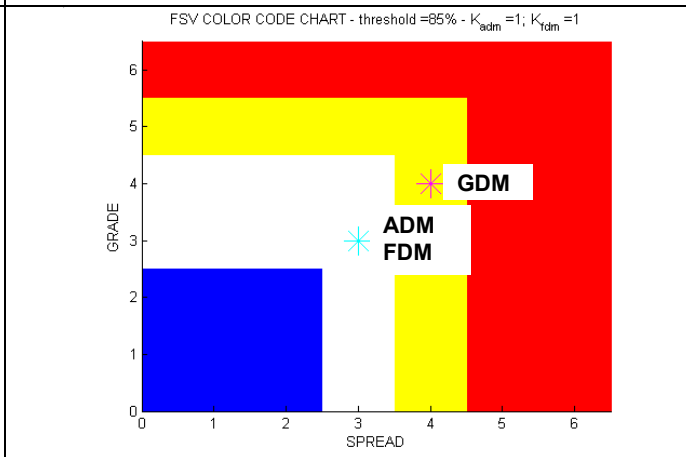


Fig. 33d – GRADE-SPREAD chart referred to Fig.

5.2 Board with printed equivalent length straight line

Considering the board with the equivalent length straight line, the transient voltage waveform across the load termination for two different mesh settings of the substrate and the transient voltage waveform across the load termination considering two different extension of the GND plane has been computed.

Substrate meshing: Fine mesh

The case with fine mesh is shown in Fig. 34. The substrate has been meshed with dense mesh lines.

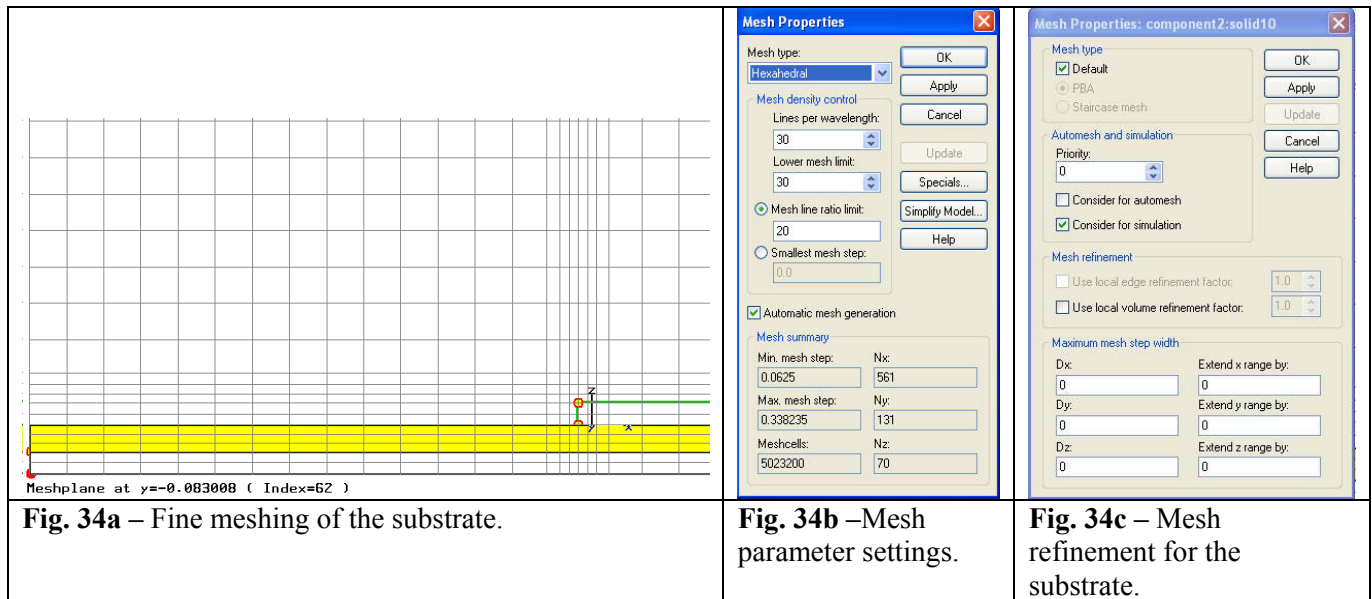


Fig. 34a – Fine meshing of the substrate.

Fig. 34b – Mesh parameter settings.

Fig. 34c – Mesh refinement for the substrate.

Substrate meshing: coarse mesh

The case with coarse mesh is shown in Fig 35. The substrate has been meshed with coarse mesh lines.

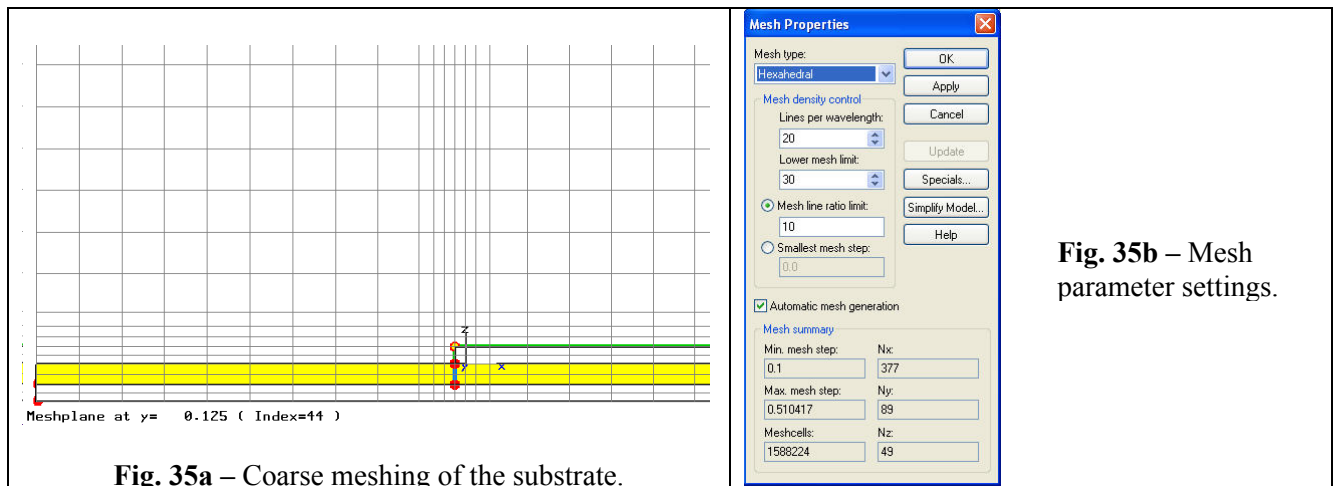


Fig. 35a – Coarse meshing of the substrate.

Fig. 35b – Mesh parameter settings.

Board with equivalent length straight line: substrate fine and coarse mesh results comparison

Fig. 36 shows the comparison, for fine and coarse mesh of the substrate, of the transient voltage waveform across the load termination for the case board with the equivalent length straight line. Fig. 37 shows the FSV comparison.

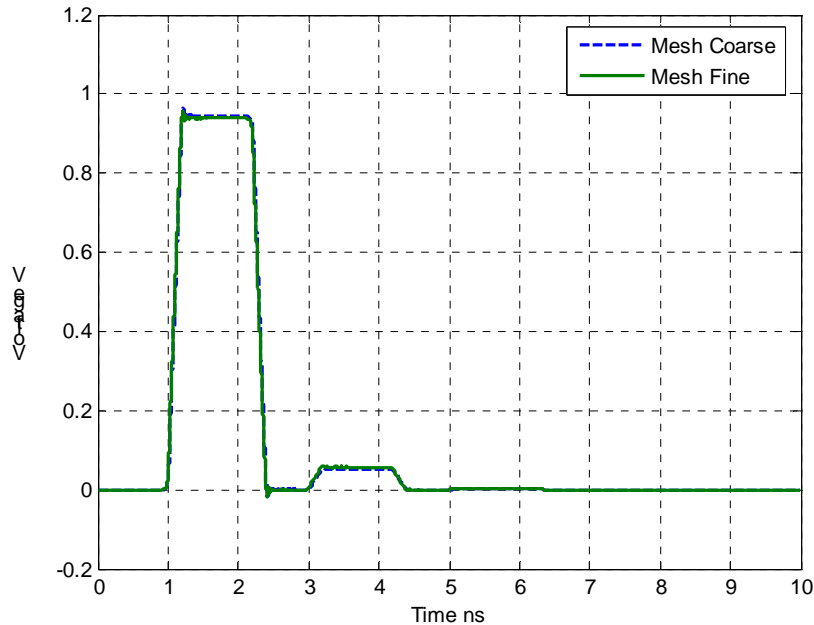
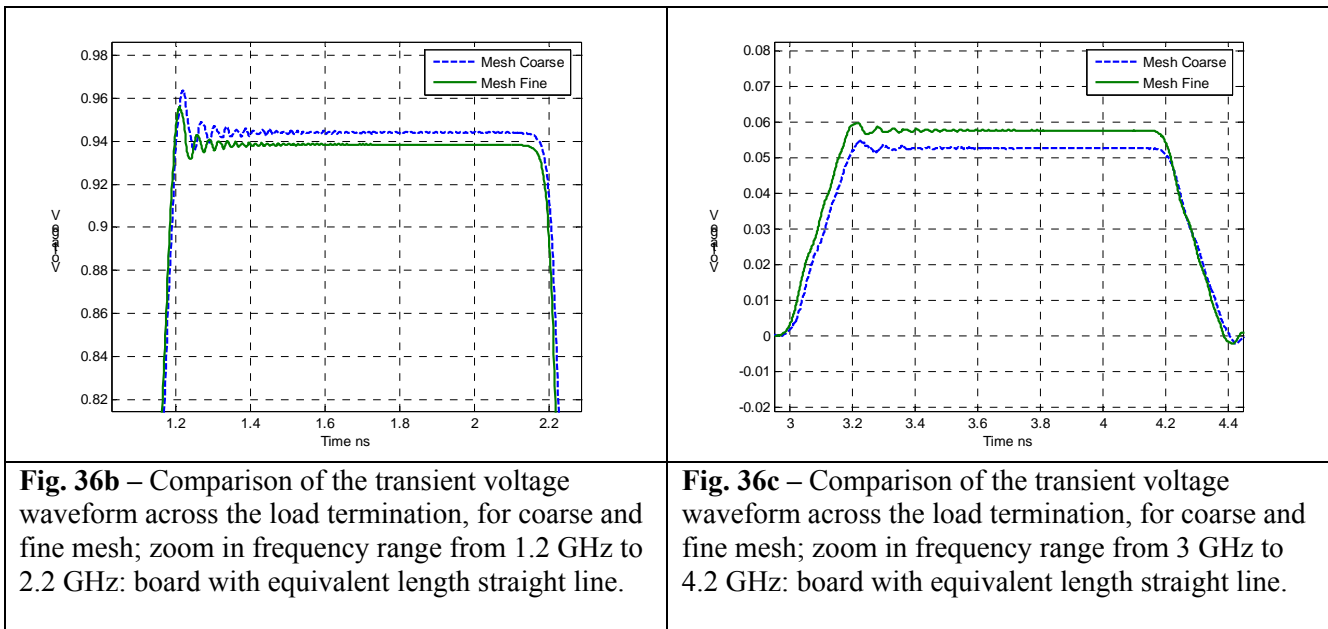


Fig. 36a – Comparison of the transient voltage waveform across the load termination: board with the equivalent length straight line.



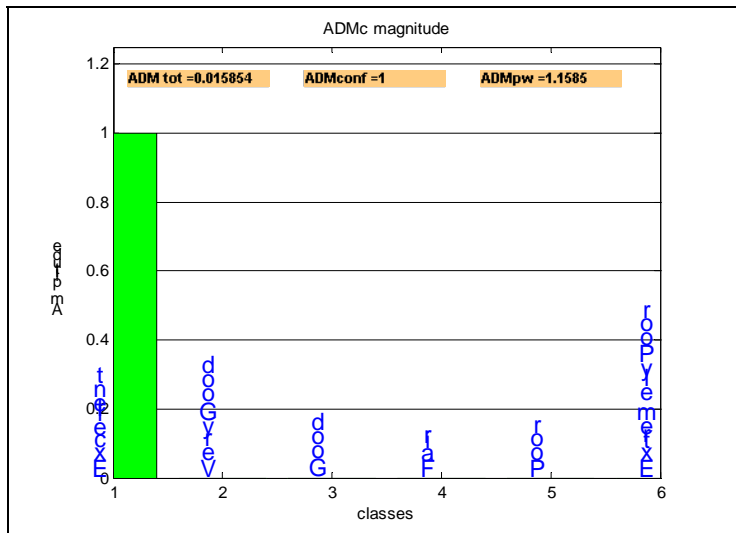


Fig. 37a – ADMc confidence diagram referred to Fig. 36.

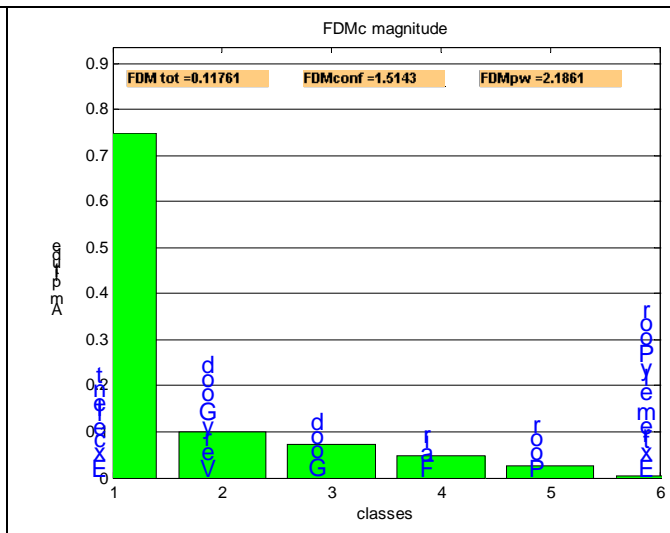


Fig. 37b – FDMc confidence diagram referred to Fig. 36.

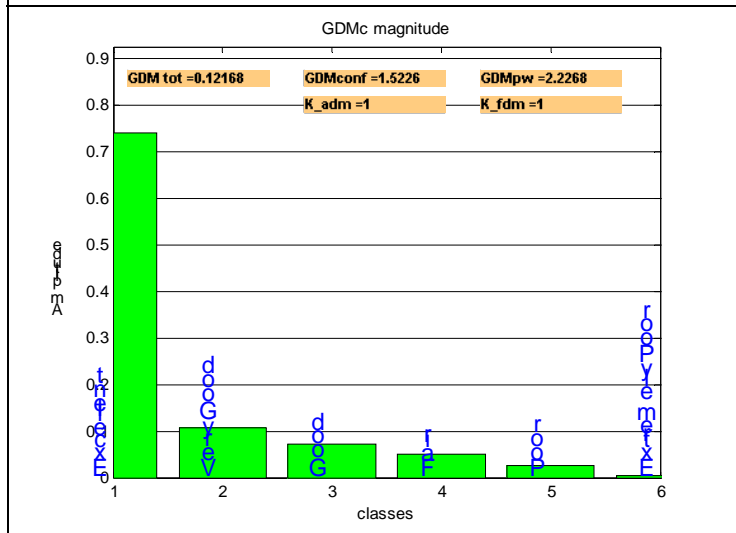


Fig. 37c – GDMc confidence diagram referred to Fig. 36.

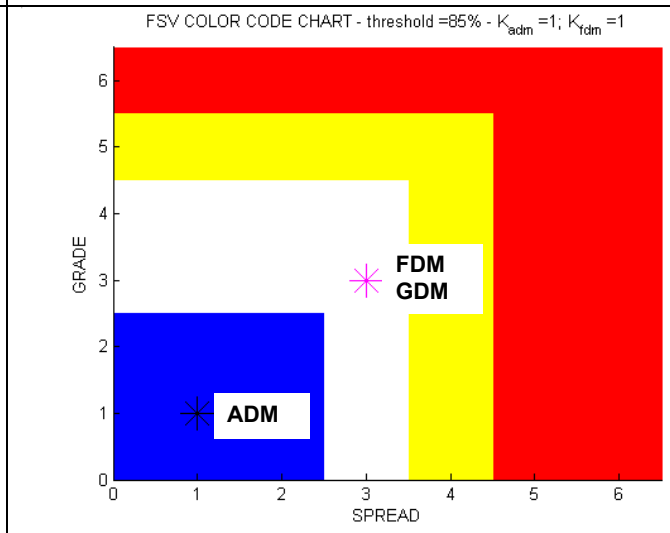


Fig. 37d – GRADE-SPREAD chart referred to Fig. 36.

5.3 Board with printed equivalent length straight line: wide GND plane

In order to investigate the effect on the result of the extension of the dimension of the reference plane and dielectric substrate, a new structure, as in Fig. 38, is considered.

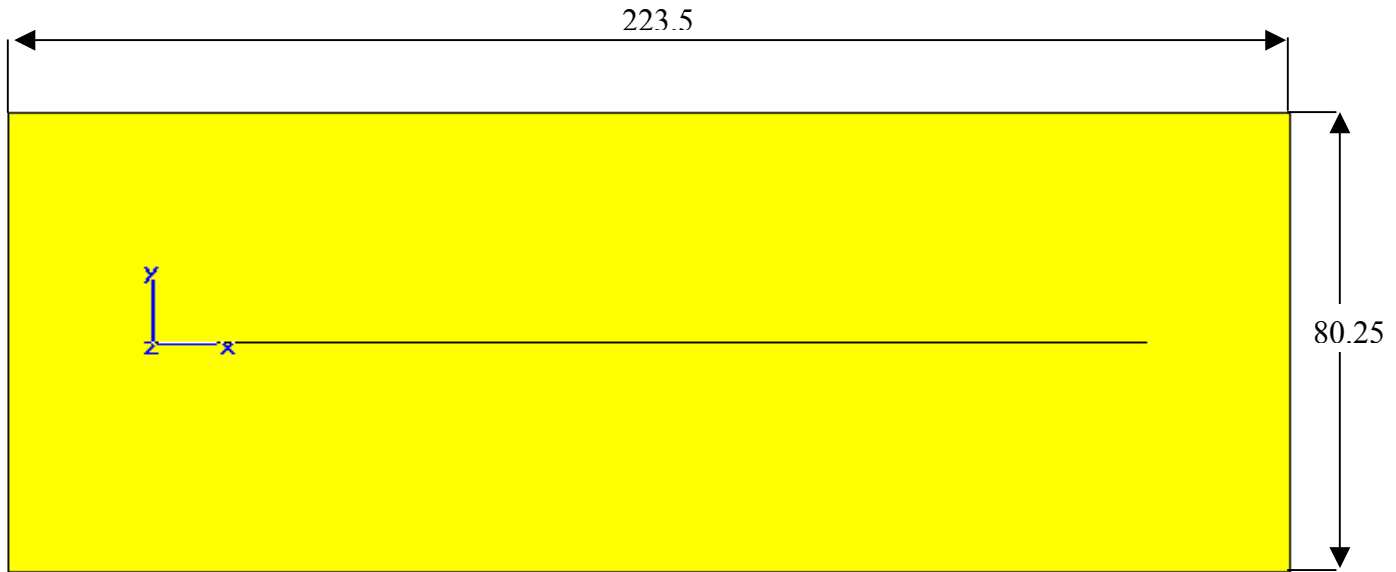


Fig. 38 – Top view: geometric dimensions of the board with printed equivalent length straight line and wide reference plane.

Equivalent Length Straight Line Model: wide reference plane (see Fig. 38) - The PCB model has the following characteristics: the reference plane is in Perfect Electric Conductor (PEC) material whose dimensions are 223.5 mm x 80.25 mm x 0.2 mm (x,y,z axis). On the PEC plane there is a dielectric substrate of FR4 whose dimensions are 223.5 mm x 80.25 mm x 0.25 mm; its dielectric permittivity is $\epsilon_r = 4.5$ and no dielectric losses are considered. The straight trace in PEC materials is placed on the dielectric substrate. The trace is simulated as a PEC material. The characteristic impedance of the line is 50 Ω .

Wide reference plane: comparison results

In Fig. 39 is shown the comparison of the transient voltage waveform across the load termination for the cases: board with equivalent length straight line and original reference plane size as shown in Fig. 28 and the case with wide reference plane as in Fig. 38. Fig. 40 show the corresponding FSV comparison.

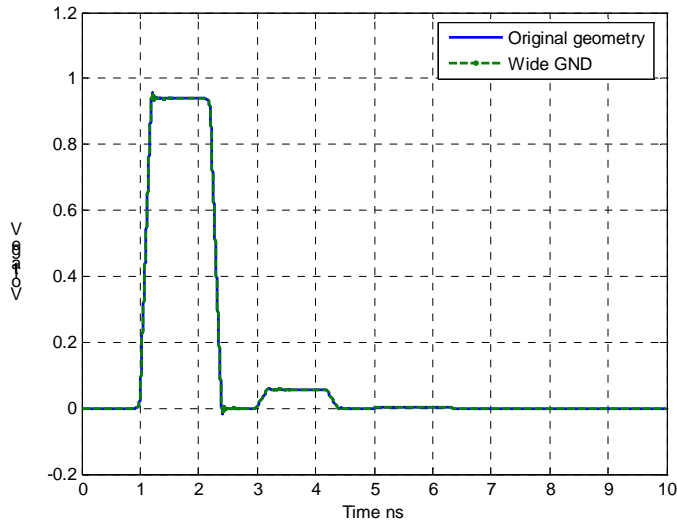


Fig. 39 – Comparison of the transient voltage waveform across the load termination: board with printed equivalent length straight line original dimensions and with wide GND plane.

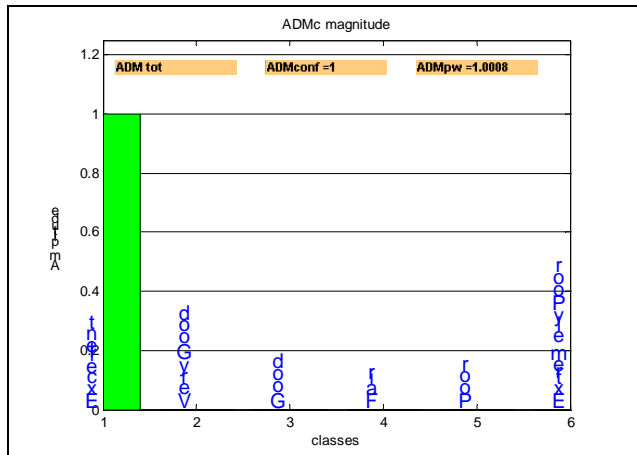


Fig. 40a - ADMc confidence diagram referred to Fig. 39.

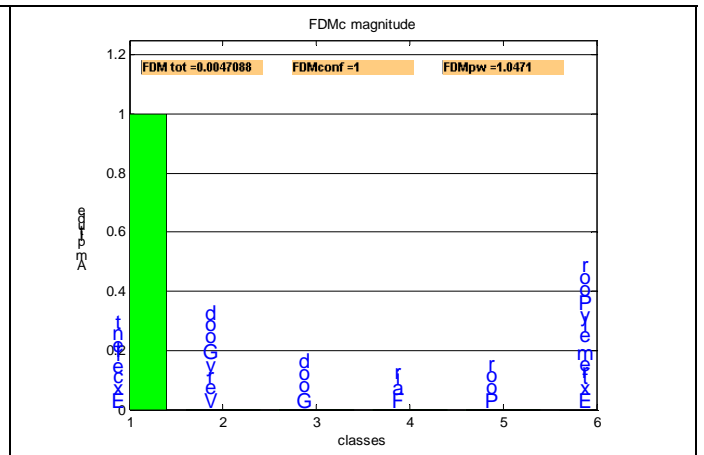


Fig. 40b - FDMc confidence diagram referred to Fig. 39.

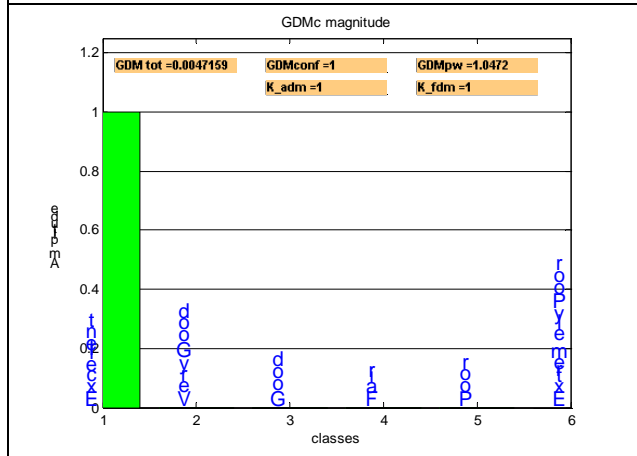


Fig. 40c - GDMc confidence diagram referred to Fig. 39.

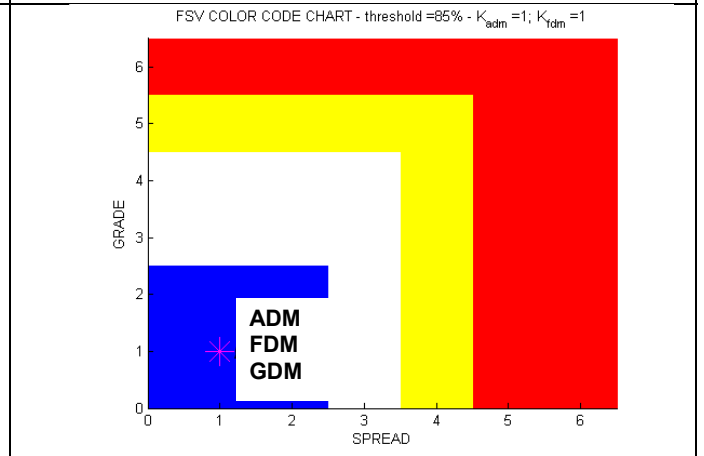


Fig. 40d – GRADE-SPREAD chart referred to Fig. 39.

5.4 Remarks

In the meander delay line model the variation of mesh parameters has a little impact on the computed results as well as in the equivalent length straight-line model in which different mesh for substrate is investigated. The extension of the GND plane has no impact on the computed transient voltage waveform at the end of the line.

6. CONCLUSION

With the proliferation of time domain electromagnetic solvers throughout microwave research and industry, their convergence properties become an issue of great practical importance. The FIT method is used in this paper to provide a general framework for the investigation of such convergence properties, along with the FSV technique, here operated to quantify the comparisons among different computational settings, so giving indications on the better choice of parameters according to the proposed aim. The sensitivity of the computed results has been investigated for different electromagnetic model varying the mesh parameter settings. The mesh is a critical feature in the numerical simulations that produce an impact on time simulations as well as an impact on the accuracy in the computed results. A proper trade-off should be always worked out.

REFERENCES

- [1] A.L.Drozdz, "Selected Methods for Validating Computational Electromagnetic Modeling Techniques", *IEEE EMC Society Newsletter*, n. 208, winter 2006.
- [2] A.L.Drozdz, "Progress on the development of standards and recommended practices for CEM computer modelling and code validation", in Proc. of 2003 IEEE Symposium on EMC, Boston, MA, August 2003.
- [3] IEEE Project 1597.1, "Standard for validation of computational electromagnetics (CEM) computer modelling and simulation", *IEEE P1597.1, Draft D1.2*, January 2005.
- [4] Computer Simulation Technology, *CST MicrowaveStudio Manual – ver. 5.1.2 -*, Vol I, II, www.cst.de.
- [5] T. Weiland, "A Discretization Method for the Solution of Maxwell's Equation for Six Component Fields", *Electronics and communication, (AEÜ)*, Vol.31 (1977), p. 116.
- [6] Martin AJM, "Quantitative data validation (automated visual evaluations)", PhD Thesis, De Montfort University, UK, 1999.
- [7] Woolfson MS, Benson TM, Christopoulos C and Duffy AP, 1995, "Quantitative Assessment of the Comparison of Electromagnetic Calculations with Experimental Data", *Applied Computational Electromagnetics Society Newsletter*, 1(1), pp 34-39.
- [8] A.P.Duffy, A.J.M.Martin, A.Orlandi, G.Antonini, T.M. Benson, M.S. Woolfson, "Feature Selective Validation (FSV) for Validation of Computational Electromagnetics (CEM) – Part I: The FSV Method", *IEEE Transactions on Electromagnetic Compatibility*, vol. 48, n.3, 2006.
- [9] A.P.Duffy, A.J.M.Martin, A.Orlandi, G.Antonini, T.M. Benson, M.S. Woolfson, "Feature Selective Validation (FSV) for Validation of Computational Electromagnetics (CEM) – Part II: Assessment of FSV Performances", *IEEE Transactions on Electromagnetic Compatibility*, vol. 48, n.3, 2006.